CANADIAN THESES ON MICROFICHE

I.S.B.N.

THESES CANADIENNES SUR MICROFICHE

National Library of Canada
Collections Development Branch

Canadian Theses on
Microfiche Service

Ottawa, Canada
K1A 0N4

Bibliothèque nationale du Canada
Direction du développement des collections

Service des thèses canadiennes
sur microfiche

NOTICE

The quality of this microfiche is heavily dependent upon the quality of the original thesis submitted for microfilming. Every effort has been made to ensure the highest quality of reproduction possible.

If pages are missing, contact the university which granted the degree.

Some pages may have indistinct print especially if the original pages were typed with a poor typewriter ribbon or if the university sent us a poor photocopy.

Previously copyrighted materials (journal articles, published tests, etc.) are not filmed.

Reproduction in full or in part of this film is governed by the Canadian Copyright Act, R.S.C. 1970, c. C-30. Please read the authorization forms which accompany this thesis.

THIS DISSERTATION
HAS BEEN MICROFILMED
EXACTLY AS RECEIVED

AVIS

La qualité de cette microfiche dépend grandement de la qualité de la thèse soumise au microfilmage. Nous avons tout fait pour assurer une qualité supérieure de reproduction.

S'il manque des pages, veuillez communiquer avec l'université qui a conféré le grade.

La qualité d'impression de certaines pages peut laisser à désirer, surtout si les pages originales ont été dactylographiées à l'aide d'un ruban usé ou si l'université nous a fait parvenir une photocopie de mauvaise qualité.

Les documents qui font déjà l'objet d'un droit d'auteur (articles de revue, examens publiés, etc.) ne sont pas microfilmés.

La reproduction, même partielle, de ce microfilm est soumise à la Loi canadienne sur le droit d'auteur, SRC 1970, c. C-30. Veuillez prendre connaissance des formules d'autorisation qui accompagnent cette thèse.

LA THÈSE A ÉTÉ
MICROFILMÉE TELLE QUE
NOUS L'AVONS REÇUE

NL-339 (r. 82/08)

Canada

83

0-315-12398-2

National Library of Canada
Bibliothèque nationale du Canada

Canadian Theses Division
Division des thèses canadiennes

Ottawa, Canada
K1A 0N4

60309

PERMISSION TO MICROFILM — AUTORISATION DE MICROFILMER

• Please print or type — Écrire en lettres moulées ou dactylographier

Full Name of Author — Nom complet de l'auteur

Raymond Doo

Date of Birth — Date de naissance
May 20, 1957

Country of Birth — Lieu de naissance
Singapore

Permanent Address — Résidence fixe
10957 - 75 Avenue
Edmonton, Alberta
Canada T6G 0G8

Title of Thesis — Titre de la thèse

Transient Temperatures in Thrust Bearings

University — Université
University of Alberta

Degree for which thesis was presented — Grade pour lequel cette thèse fut présentée
M. Sc. (Mechanical Engineering)

Year this degree conferred — Année d'obtention de ce grade
Fall 1982

Name of Supervisor — Nom du directeur de thèse
Dr. C. M. Rodkiewicz

Permission is hereby granted to the NATIONAL LIBRARY OF CANADA to microfilm this thesis and to lend or sell copies of the film.

The author reserves other publication rights, and neither the thesis nor extensive extracts from it may be printed or otherwise reproduced without the author's written permission.

L'autorisation est, par la présente, accordée à la BIBLIOTHÈQUE NATIONALE DU CANADA de microfilmer cette thèse et de prêter ou de vendre des exemplaires du film.

L'auteur se réserve les autres droits de publication; ni la thèse ni de longs extraits de celle-ci ne doivent être imprimés ou autrement reproduits sans l'autorisation écrite de l'auteur.

Date
Oct. 13, 1982

Signature
Raymond Doo

NL-91 (4/77)

THE UNIVERSITY OF ALBERTA

Transient Temperatures in Thrust Bearings

by

© Raymond Doo

A THESIS

SUBMITTED TO THE FACULTY OF GRADUATE STUDIES AND RESEARCH

IN PARTIAL FULFILMENT OF THE REQUIREMENTS FOR THE DEGREE

OF Master of Science

Department of Mechanical Engineering

EDMONTON, ALBERTA

Fall 1982

Microfilming

THE UNIVERSITY OF ALBERTA

RELEASE FORM

NAME OF AUTHOR Raymond Doo

TITLE OF THESIS Transient Temperatures in Thrust Bearings

DEGREE FOR WHICH THESIS WAS PRESENTED Master of Science

YEAR THIS DEGREE GRANTED 1982

Permission is hereby granted to THE UNIVERSITY OF ALBERTA LIBRARY to reproduce single copies of this thesis and to lend or sell such copies for private, scholarly or scientific research purposes only.

The author reserves other publication rights, and neither the thesis nor extensive extracts from it may be printed or otherwise reproduced without the author's written permission.

(SIGNED) ...Raymond Doo.....

PERMANENT ADDRESS:

10957 - 75 Avenue

Edmonton, Alberta

Canada T6G 0G8

DATED September 14, 1982

THE UNIVERSITY OF ALBERTA

FACULTY OF GRADUATE STUDIES AND RESEARCH

The undersigned certify that they have read, and recommend to the Faculty of Graduate Studies and Research, for acceptance, a thesis entitled Transient Temperatures in Thrust Bearings submitted by Raymond Doo in partial fulfilment of the requirements for the degree of Master of Science in Mechanical Engineering.

C.A. Rodkiewicz

Supervisor

J.C. Kennedy

M. Goodman

Date 12th Oct. 1982

SUMMARY

Studies were made on a thrust bearing with two different slider boundary conditions, namely, constant temperature and adiabatic surface. This study was based on the transient momentum and energy equations. A number of numerical simulations were performed using different bearing ratios and Prandtl and Eckert numbers.

It was found that the location of maximum temperature depended on the bearing ratio. For a bearing ratio of 2.2, maximum temperature was near the slider. For a bearing ratio of 1.5, maximum temperature was near the stationary surface. Temperature computations were carried out until transient values were acceptably close to the steady-state values.

Acknowledgments

The author is deeply grateful to Dr. C. M. Rodkiewicz for his help in the formulation of the problem and his continuing interest in this work. The author wishes to thank his sister, Irene, for her untiring efforts in the preparation of this thesis.

TABLE OF CONTENTS

CHAPTER		PAGE
I.	INTRODUCTION	1
	Background to the problem	1
	Present study	2
II.	TRANSIENT MOMENTUM AND TEMPERATURE EQUATIONS	3
	Governing equations	3
	Numerical method	6
III.	STEADY-STATE MOMENTUM AND TEMPERATURE EQUATIONS	13
	Governing equations	13
	Numerical method	15
IV.	DISCUSSION OF RESULTS	17
	Transient temperature profiles for the case of	
	i) constant slider temperature	17
	ii) an adiabatic slider	25
V.	CONCLUSIONS	29
	REFERENCES	68
	BIBLIOGRAPHY	70

LIST OF TABLES

Table		Page
I.	Bearing ratios, Prandtl and Eckert numbers used in simulations	12

LIST OF FIGURES

Figure		Page
1.	Coordinate system of thrust bearing	4
2.	Computational molecule (x position is fixed)	8
3.	Transient temperature distribution at $x^* = 0.1$ for K = 2.2 (constant slider temperature)	30
4.	Transient temperature distribution at $x^* = 0.4$ for K = 2.2 (constant slider temperature)	31
5.	Transient temperature distribution at $x^* = 0.7$ for K = 2.2 (constant slider temperature)	32
6.	Transient temperature distribution at $x^* = 1.0$ for K = 2.2 (constant slider temperature)	33
7.	Transient temperature distribution at $x^* = 0.1$ for K = 1.5 (constant slider temperature)	34
8.	Transient temperature distribution at $x^* = 0.4$ for K = 1.5 (constant slider temperature)	35
9.	Transient temperature distribution at $x^* = 0.7$ for K = 1.5 (constant slider temperature)	36
10.	Transient temperature distribution at $x^* = 1.0$ for K = 1.5 (constant slider temperature)	37
11.	Transient velocity distribution at $x^* = 0.1$ for K = 2.2	38
12.	Transient velocity distribution at $x^* = 0.4$ for K = 2.2	39
13.	Transient velocity distribution at $x^* = 0.7$ for K = 2.2	40
14.	Transient velocity distribution at $x^* = 1.0$ for K = 2.2	41
15.	Transient velocity distribution at $x^* = 0.1$ for K = 1.5	42
16.	Transient velocity distribution at $x^* = 0.4$ for K = 1.5	43
17.	Transient velocity distribution at $x^* = 0.7$ for K = 1.5	44

18. Transient velocity distribution at $x^* = 1.0$ for $K = 1.5$ 45

19. Transient shear stress distribution at $x^* = 0.1$ for $K = 2.2$ 46

20. Transient shear stress distribution at $x^* = 0.4$ for $K = 2.2$ 47

21. Transient shear stress distribution at $x^* = 0.7$ for $K = 2.2$ 48

22. Transient shear stress distribution at $x^* = 1.0$ for $K = 2.2$ 49

23. Transient shear stress distribution at $x^* = 0.1$ for $K = 1.5$ 50

24. Transient shear stress distribution at $x^* = 0.4$ for $K = 1.5$ 51

25. Transient shear stress distribution at $x^* = 0.7$ for $K = 1.5$ 52

26. Transient shear stress distribution at $x^* = 1.0$ for $K = 1.5$ 53

27. Pressure distribution for $K = 2.2$ 54

28. Pressure distribution for $K = 1.5$ 55

29. Transient temperature distribution at $x^* = 0.1$ for $K = 2.2$ (adiabatic slider) 56

30. Transient temperature distribution at $x^* = 0.4$ for $K = 2.2$ (adiabatic slider) 57

31. Transient temperature distribution at $x^* = 0.7$ for $K = 2.2$ (adiabatic slider) 58

32. Transient temperature distribution at $x^* = 1.0$ for $K = 2.2$ (adiabatic slider) 59

33. Transient temperature distribution at $x^* = 0.1$ for $K = 1.5$ (adiabatic slider) 60

34. Transient temperature distribution at $x^* = 0.4$ for $K = 1.5$ (adiabatic slider) 61

35. Transient temperature distribution at $x^* = 0.7$ for $K = 1.5$ (adiabatic slider) 62

36. Transient temperature distribution at $x^* = 1.0$ for $K = 1.5$ (adiabatic slider) 63

37. Convection term along bearing as a function of y^* ($t^* = 3.0$, $K = 2.2$, adiabatic case) 64

38. Convection term across bearing as a function of y^* ($t^* = 3.0$, $K = 2.2$, adiabatic case) 65

39. Conduction term as a function of y^* ($t^* = 3.0$, $K = 2.2$, adiabatic case) 66

40. Viscous term as a function of y^* ($t^* = 3.0$, $K = 2.2$, adiabatic case) 67

NOMENCLATURE

a	= acceleration of slider
a^*	= $ah_o^3/(B\nu^2)$ = dimensionless acceleration
a,b,c,d	= coefficients used in numerical method
B	= length of slider in direction of motion
Cp	= specific heat of lubricant at constant pressure
E	= $(B\nu/h_o^2)^2/(Cp\ T_s)$ = a type of Eckert number
h	= film thickness
h_i	= inlet film thickness
h_o	= outlet film thickness
h^*	= h/h_o = dimensionless film thickness
i,j,k	= numerical method equivalents of x, y, and t respectively
K	= h_i/h_o = bearing ratio
M,N	= number of computational points in the x and y directions respectively
p	= gauge pressure
p^*	= $p\rho h_o^3/(B\mu)^2$ = dimensionless gauge pressure
P	= $Cp\mu/\kappa$ = Prandtl number
Q	= flow rate per unit width
Q^*	= $Qh_o/(B\nu)$ = dimensionless flow rate
t	= time
t^*	= $\nu t/h_o^2$ = dimensionless time
T(x, y)	= temperature of lubricant at position (x, y)
T_s	= constant surface temperature
T^*	= T/T_s = dimensionless temperature of lubricant
u	= velocity in x-direction

u^* = $uh_o^2/(B\nu)$ = dimensionless velocity in x-direction

U = velocity of slider

U^* = $Uh_o^2/(B\nu)$ = dimensionless velocity of slider

v = velocity in y-direction

v^* = vh_o/ν = dimensionless velocity in y-direction

x = coordinate along the bearing, $0 \leq x \leq B$

x^* = x/B = dimensionless x-coordinate

y = coordinate across the bearing, $0 \leq y \leq h$

y^* = y/h_o = dimensionless y-coordinate

κ = thermal conductivity

μ = absolute viscosity

ν = kinematic viscosity

ρ = density of lubricant

CHAPTER I

INTRODUCTION

Background to the problem

Numerous studies have been done on steady-state momentum and energy equations in connection with thrust bearings. Hahn and Kettleborough [1] used these equations to solve for pressure and temperature distributions in a thrust bearing. The effects of inertia terms on pressure and load capacity, and the effect of convective terms on temperatures at the surfaces were investigated by Rodkiewicz and Anwar [2]. Other studies concentrated on varying temperatures at the surfaces and different bearing ratios [3]; keeping the two surfaces adiabatic [4]; a different numerical procedure for calculation of flow in finite width bearing films [5].

There have been a number of studies done on the transient momentum equation. One of the earliest works was done by Ladanyi [6] who investigated the effects of acceleration on performance characteristics in slider and journal bearings. Lyman and Saibel [7] did an analytical study of the transient pressures in an infinite slider but did not assume that acceleration was proportional to the distance across the bearing as in the previous paper. A more recent paper by Venkateswarlu and Rodkiewicz [8] studied the development of transient load capacity and drag for three functional variations of velocity.

Present study

This study is concerned with transient temperatures in a thrust bearing. The solution of the transient momentum equation is used to solve for the temperature distribution in the bearing. As far as this author knows, this is probably the first study made on the transient energy equation. This research was done for a specific range of parameters. Therefore, it is recommended that further studies be made on the transient energy equation.

CHAPTER II

TRANSIENT MOMENTUM AND ENERGY EQUATIONS

Governing equations

The thrust bearing configuration considered for this analysis is shown in Fig. 1. The governing equations, assuming an incompressible fluid of constant properties, or the two-dimensional bearing are

$$\rho\left(\frac{\partial u}{\partial t} + u\frac{\partial u}{\partial x} + v\frac{\partial u}{\partial y}\right) = -\frac{\partial p}{\partial x} + \mu\frac{\partial^2 u}{\partial y^2} \tag{1}$$

$$\frac{\partial u}{\partial x} + \frac{\partial v}{\partial y} = 0 \tag{2}$$

$$\rho Cp\left(\frac{\partial T}{\partial t} + u\frac{\partial T}{\partial x} + v\frac{\partial T}{\partial y}\right) = \kappa\frac{\partial^2 T}{\partial y^2} + \mu\left(\frac{\partial u}{\partial y}\right)^2 \tag{3}$$

with the following velocity and pressure boundary conditions

$$\begin{aligned} &u(x,h,t) = u(x,y,0) = 0 \\ &v(x,h,t) = v(x,0,t) = v(x,y,0) = 0 \\ &p(0,t) = p(B,t) = 0 \\ &u(x,0,t) = U = at \end{aligned} \tag{4}$$

and the following two cases of temperature boundary conditions

$$\begin{aligned} &T(x,h,t) = T(x,y,0) = T(0,y,t) = T_s \\ &T(x,0,t) = T_s \end{aligned} \tag{5}$$

or

$$\begin{aligned} &T(x,h,t) = T(x,y,0) = T(0,y,t) = T_s \\ &\frac{\partial T}{\partial y}(x,0,t) = 0 \end{aligned} \tag{6}$$

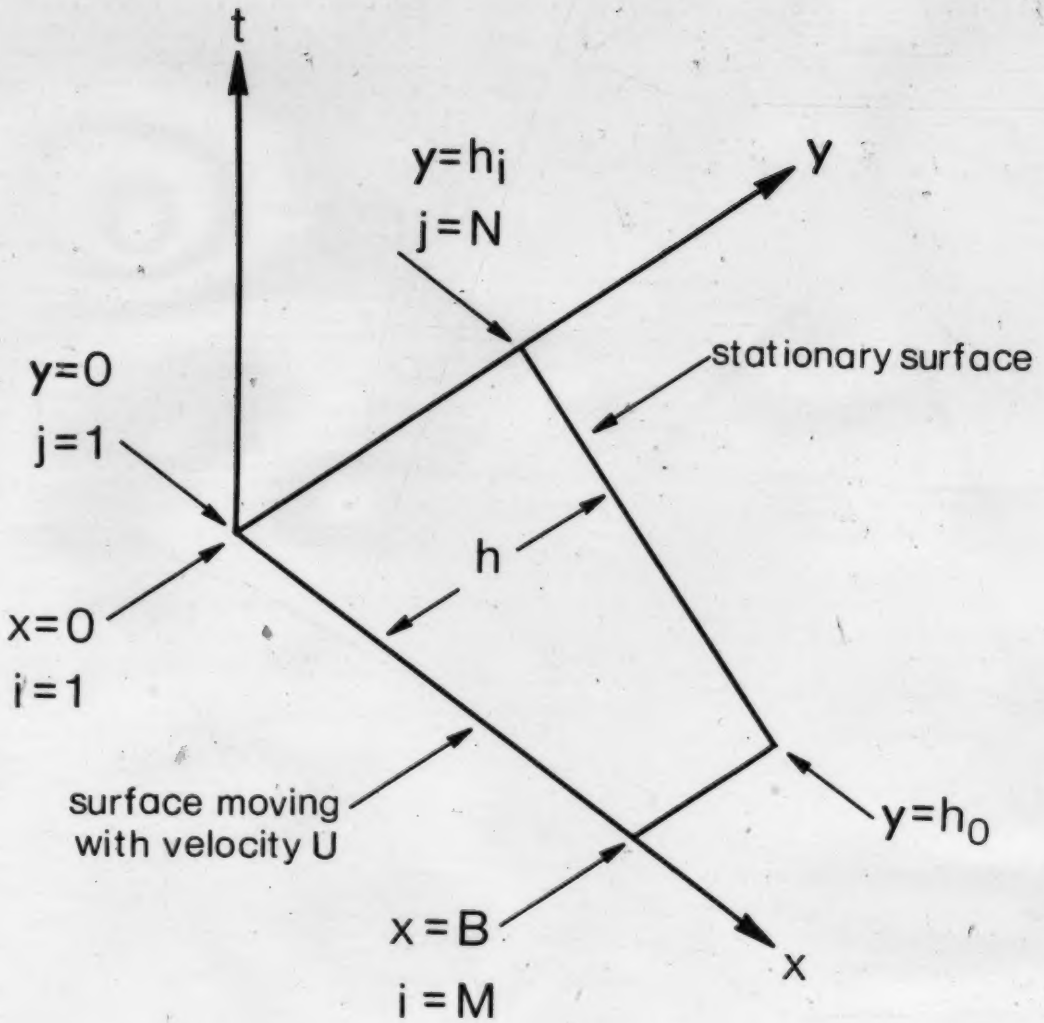

Fig. 1. Coordinate system of thrust bearing

The transient momentum equation (1) with the boundary conditions (4) have been used in ref.[8,9]. In these papers and in the present study, U = at where a is the acceleration of the slider. This means that the slider is stationary when the time is zero. This study will be concentrated on the transient energy equation (3).

Equations (1) and (2) can be combined and together with the energy equation (3) can be written in dimensionless form as follows

$$\frac{\partial u^*}{\partial t^*} - u^*\frac{\partial v^*}{\partial y^*} + v^*\frac{\partial u^*}{\partial y^*} = -\frac{\partial p^*}{\partial x^*} + \frac{\partial^2 u^*}{\partial y^{*2}} \tag{7}$$

$$\frac{\partial T^*}{\partial t^*} + u^*\frac{\partial T^*}{\partial x^*} + v^*\frac{\partial T^*}{\partial y^*} = \frac{1}{P}\frac{\partial^2 T^*}{\partial y^{*2}} + E\left(\frac{\partial u^*}{\partial y^*}\right)^2 \tag{8}$$

The corresponding boundary conditions become

$$\begin{aligned} &u^*(x^*,h^*,t^*) = u^*(x^*,y^*,0) = 0 \\ &v^*(x^*,h^*,t^*) = v^*(x^*,0,t^*) = v^*(x^*,y^*,0) = 0 \\ &p^*(0,t^*) = p^*(1,t^*) = 0 \\ &u^*(x^*,0,t^*) = U^* = a^*t^* \end{aligned} \tag{9}$$

and

$$\begin{aligned} &T^*(x^*,h^*,t^*) = T^*(x^*,y^*,0) = T^*(0,y^*,t^*) = 1.0 \\ &T^*(x^*,0,t^*) = 1.0 \end{aligned} \tag{10}$$

or

$$\begin{aligned} &T^*(x^*,h^*,t^*) = T^*(x^*,y^*,0) = T^*(0,y^*,t^*) = 1.0 \\ &\frac{\partial T^*}{\partial y^*}(x^*,0,t^*) = 0 \end{aligned} \tag{11}$$

In the boundary conditions (9), (10), (11), the quantity $h^*(x^*)$ describes the shape of the stationary part

of the thrust bearing with reference to the moving slider. The shape assumed is for a linear bearing, namely

$$h^*(x^*) = K + (1 - K)\, x^* \tag{12}$$

The solution of equation (7) yields the velocity distribution in the bearing at time t^*. Since the fluid properties are constant, the solution of equation (7) is uncoupled from equation (8) and can be solved independently. The velocity distribution at time t^* is used in equation (8) to solve for the temperature distribution in the oil film.

Numerical method

The dimensionless differentials in equations (7) and (8) can be written in finite-difference form as follows

$$u^*_{i,j,k} = u^*_{i,j,k-1} + \left[\frac{\Delta t^* u^*}{2\Delta y^*}_{i,j,k-1} \left(v^*_{i,j+1,k-1} - v^*_{i,j-1,k-1}\right)\right.$$

$$\left. - \frac{\Delta t^* v^*}{2\Delta y^*}_{i,j,k-1} \left(u^*_{i,j+1,k-1} - u^*_{i,j-1,k-1}\right)\right] \tag{13}$$

$$- \Delta t^* \frac{\partial p^*}{\partial x^*}\Big|_{i,k-1} + \frac{\Delta t^*}{(\Delta y^*)^2} \left(u^*_{i,j+1,k-1} - 2u^*_{i,j,k-1} + u^*_{i,j-1,k-1}\right)$$

and

$$a_{i,j}\, T^*_{i,j-1,k} + b_{i,j}\, T^*_{i,j,k} + c_{i,j}\, T^*_{i,j+1,k} = d_{i,j} \qquad (14)$$

where

$$a_{i,j} = -\frac{\Delta t^*}{2\Delta y^*} v^*_{i,j,k} - \frac{\Delta t^*}{(\Delta y^*)^2} P^{-1}$$

$$b_{i,j} = 1 + \frac{\Delta t^* u^*}{\Delta x^*}_{i,j,k} + \frac{2\Delta t^*}{(\Delta y^*)^2} P^{-1} \qquad (15)$$

$$c_{i,j} = \frac{\Delta t^* v^*}{2\Delta y^*}_{i,j,k} - \frac{\Delta t^*}{(\Delta y^*)^2} P^{-1}$$

$$d_{i,j} = \left(\frac{\Delta t^* u^*}{\Delta x^*}_{i,j,k}\right) T^*_{i-1,j,k} + T^*_{i,j,k-1}$$

$$+ \frac{\Delta t^*}{4(\Delta y^*)^2} E \left(u^*_{i,j+1,k} - u^*_{i,j-1,k} \right)^2$$

As shown in Figs. 1 and 2, h and B are divided into a finite number of uniform N - 1 and M - 1 intervals, respectively, and x^* has been replaced by i, y^* by j, and t^* by k. The origin is fixed with respect to the stationary surface. Initially, $u^*(i,j,1) = 0$ for the entire bearing. When k = 2, the bearing acquires a velocity $u^*(i,j,2) = a^*t^*$ for $j = 1$ and $u^*(i,j,2) = 0$ for $j \neq 1$. An arbitrary value of $(\partial p^*/\partial x^*)_m$ is used to start off the calculations at i = M. $u^*(M,j,k)$ can be calculated for all values of j and

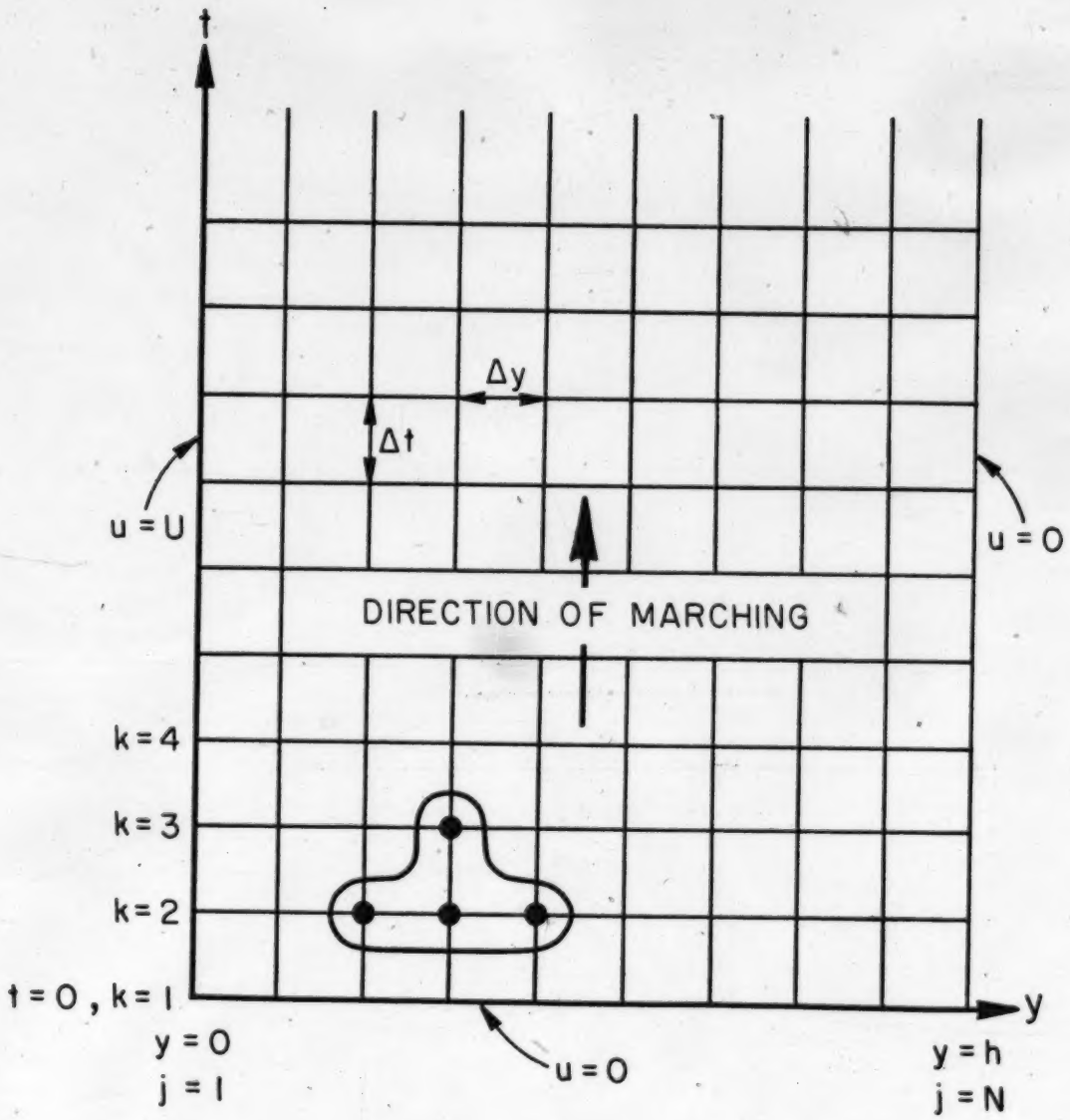

Fig. 2. Computational molecule (x position is fixed)

$k = 3$ from equation (13). In the next step, the dimensionless flow rate Q_m^* corresponding to

$$Q^* = \int_0^{h^*} u^* dy^* \tag{16}$$

is obtained using Simpson's rule on the values $u^*(M,1,k)$, ..., $u^*(M,N,k)$. Then, i is decreased by 1, $i = i - 1$, and the computation of $u^*(i,1,k)$, ..., $u^*(i,N,k)$ and Q_i^* is performed assuming a value for $(\partial p^*/\partial x^*)_i$. It is known that Q^*, if correct, should be a function of time only and must not vary with changing i or x^*. Therefore, the computed flow rate at i and M must be equal. If there is a significant difference, a new value of $(\partial p^*/\partial x^*)_i$ is used. The pressure gradient at i is adjusted until a satisfactory Q_i^* is obtained. It is found that the relationship between $\partial p^*/\partial x^*$ and Q^* is approximately linear. Therefore, a better approximation of $\partial p^*/\partial x^*$ can be obtained. The final value of pressure gradient at i is found by iteratively correcting the previous value.

Once $(\partial p^*/\partial x^*)_1$, ..., $(\partial p^*/\partial x^*)_m$ are known, the integral

$$\int_0^1 \frac{\partial p^*}{\partial x^*} dx^* = p_m^* \tag{17}$$

is performed using Simpson's rule over the $M - 1$ intervals of $1/(M - 1)$ each. It must be equal to zero in order to satisfy the boundary conditions (9). If it is not so, the value of $(\partial p^*/\partial x^*)_m$ must be adjusted and the computation

of u^*, Q^* and $\partial p^*/\partial x^*$ is repeated. This process is repeated until the integral is close to zero. It is also found that the relation between $(\partial p^*/\partial x^*)_m$ and p^*_m is approximately linear and therefore a better approximation for $(\partial p^*/\partial x^*)_m$ is possible. The pressure distribution can be determined from the following equation

$$p^*(i,j,k) = \int_0^{x^*} \frac{\partial}{\partial x^*} \{ p^*(i,j,k) \} \, dx^* \qquad (18)$$

Once the velocity distribution is known at k = 3, the temperature distribution can be calculated from equation (14) with its coefficients in equation (15).

The temperature distribution is solved iteratively by using the Gauss-Seidel method with relaxation. Equation (14) together with particular Prandtl and Eckert numbers are solved by this method. Iteration is stopped when the present set of values are in close agreement with the previous set. The calculations are based on the assumption that one upstream solution is known. Formulation of equation (14) is based on a 4-point computational molecule

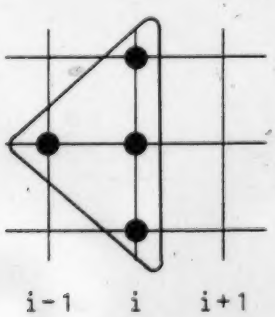

Therefore, the calculations proceed from the entrance

where i = 1 to the exit where i = M, in one unit increments. The first set of $T^*(1,j,k)$ for j = 1, ..., N is known, as shown in equation (10). Note that the computation of temperature goes from the entrance (i = 1) to the exit (i = M) which is exactly opposite to the way velocity is calculated. After a satisfactory set of temperatures have been calculated, k can be incremented and the computation can be repeated for the new time interval.

This procedure has been programmed in double precision on the Amdahl 470/V8 computer. The simulation has been performed for a number of bearing ratios and Prandtl and Eckert numbers. A single simulation of the preceding problem took approximately 130 seconds of central processing time. The lubrication oil used has the following properties (at 40°C):

$$\begin{aligned} Cp &= 1.68\ kJ/kg°K & \kappa &= 0.117\ W/m°K \\ \mu &= 0.008288\ Ns/m^2 & \nu &= 9.45 \times 10^{-6} m^2/s \\ \rho &= 877\ kg/m^3 & P &= 119 \\ T_s &= 313°K \end{aligned} \qquad [10]$$

The dimensions of the thrust bearing are as follows:

$$B = 0.0914\ m \qquad h_o = 64.62 \times 10^{-6} m$$

The Eckert number can be calculated from the above data. A comparison between the type of Eckert number used here and other Eckert numbers used in ref.[1,2,3] would show

that the slider velocity, U, does not appear in the former. For this study and others [8,9], variables that are used in dimensionless constants must not vary with time. Hence, the slider velocity which varies with time has been replaced by suitable time-invariant variables. The combinations used are shown in Table I.

Constant slider temperature		
K	Prandtl	Eckert
2.2	119	0.08140874
1.5	119	0.08140874
Adiabatic slider		
K	Prandtl	Eckert
2.2	119	0.08140874
1.5	119	0.08140874

Table I Bearing ratios, Prandtl and Eckert numbers used in simulations

CHAPTER III

STEADY-STATE MOMENTUM AND ENERGY EQUATIONS

Governing equations

The thrust bearing configuration considered in the steady-state analysis of momentum and energy equations is similar to Fig. 1 except for the absence of the time axis. The governing equations for a two-dimensional bearing of constant properties are as follows

$$\rho\left(u\frac{\partial u}{\partial x} + v\frac{\partial u}{\partial y} \right) = -\frac{dp}{dx} + \mu\frac{\partial^2 u}{\partial y^2} \tag{19}$$

$$\frac{\partial u}{\partial x} + \frac{\partial v}{\partial y} = 0 \tag{20}$$

$$\rho Cp\left(u\frac{\partial T}{\partial x} + v\frac{\partial T}{\partial y} \right) = \kappa\frac{\partial^2 T}{\partial y^2} + \mu\left(\frac{\partial u}{\partial y} \right)^2 \tag{21}$$

with the following velocity and pressure boundary conditions

$$\begin{aligned} &u(x,h) = v(x,h) = v(x,0) = 0 \\ &u(x,0) = U, \quad p(0) = p(B) = 0 \end{aligned} \tag{22}$$

and the following two cases of temperature boundary conditions

$$T(0,y) = T(x,h) = T(x,0) = T_s \tag{23}$$

or

$$T(0,y) = T(x,h) = T_s, \qquad \left.\frac{\partial T}{\partial y}\right|_{y=0} = 0 \tag{24}$$

Equations (19) and (20) can be combined and together with the energy equation (21) can be written in dimensionless form as follows

$$- u^* \frac{\partial v^*}{\partial x^*} + v^* \frac{\partial u^*}{\partial y^*} = - \frac{dp^*}{dx^*} + \frac{\partial^2 u^*}{\partial y^{*2}} \tag{25}$$

$$u^* \frac{\partial T^*}{\partial x^*} + v^* \frac{\partial T^*}{\partial y^*} = \frac{1}{P} \frac{\partial^2 T^*}{\partial y^{*2}} + E \left(\frac{\partial u^*}{\partial y^*} \right)^2 \tag{26}$$

The corresponding boundary conditions become

$$u^*(x^*,h^*) = v^*(x^*,h^*) = v^*(x^*,0) = 0$$
$$u^*(x^*,0) = U^*, \qquad p^*(0) = p^*(1) = 0 \tag{27}$$

and

$$T^*(0,y^*) = T^*(x^*,h^*) = T^*(x^*,0) = 1.0 \tag{28}$$

or

$$T^*(0,y^*) = T^*(x^*,h^*) = 1.0, \left. \frac{\partial T^*}{\partial y^*} \right|_{y^* = 0} = 0 \tag{29}$$

In the boundary conditions (27), (28), (29), the quantity $h^*(x^*)$ describes the shape of the stationary part of the thrust bearing with reference to the moving slider. The shape assumed is for a linear bearing as given by equation (12). The solution of equation (25) is uncoupled from equation (26) because of the assumption that fluid properties are constant. Therefore, equation (25) can be solved independently to yield the velocity distribution in the thrust bearing. The results are used in equation (26) to solve for the temperature field in the lubricating film.

Numerical method

The differentials in equations (22) and (23) can be written in finite difference form as follows

$$u^*_{i,j-1}\left(\frac{2}{\Delta y^*} + v^*_{i,j}\right) + u^*_{i,j}\left(v^*_{i,j+1} - v^*_{i,j-1} - \frac{4}{\Delta y^*}\right) + u^*_{i,j+1}\left(\frac{2}{\Delta y^*} - v^*_{i,j}\right) = 2\Delta y^* \left.\frac{dp^*}{dx^*}\right|_i \tag{30}$$

and

$$T^*_{i,j-1}\left(-\frac{1}{2\Delta y^*} v^*_{i,j} - \frac{1}{P\Delta y^{*2}}\right) + T^*_{i,j}\left(\frac{1}{\Delta x^*} u^*_{i,j} + \frac{2}{P\Delta y^{*2}}\right) + T^*_{i,j+1}\left(\frac{1}{2\Delta y^*} v^*_{i,j} - \frac{1}{P\Delta y^{*2}}\right) = E\left(\frac{u^*_{i,j+1} - u^*_{i,j-1}}{2\Delta y^*}\right)^2 + u^*_{i,j}\frac{T^*_{i,j} - T^*_{i-1,j}}{\Delta x^*} \tag{31}$$

The computational grid is the same as before. For the steady-state calculations, the time variable does not appear. An initial set of starting values for the velocities in the bearing was generated from a program using equation (22) without the inertia terms. These values will serve as the initial guess to the full equation (22). To start the iterative process, an arbitrary value of $(dp^*/dx^*)_m$ is

guessed. The value used must be negative because of the boundary condition (22).

Using the initial pressure gradient at M, and starting with i = M, $u^*(M,j)$, j = 1, ..., N the initial velocity estimates can be calculated from equation (30) using the Gauss-Seidel method with relaxation. The iteration is stopped when the present set of values are in close agreement with the previous set of values. The rest of the numerical procedure is quite similar to that used for the transient equations. Any references to time is ignored.

The final velocity distributions are saved on computer files. These values are then used in the energy equation (31) together with the appropriate Prandtl and Eckert number (Table I). The iterative technique used is again the Gauss-Seidel method with relaxation. Iteration is terminated when the present set of temperatures are in close agreement with the previous set.

A single simulation of the steady-state equations took approximately 20 seconds of central processing time. The programs used to solve the equations have been written in double precision on the Amdahl 470/V8 computer.

CHAPTER IV

DISCUSSION OF RESULTS

Transient temperature profiles for the case of constant slider temperature

Graphs have been drawn for bearing ratios ,K, of 1.5 and 2.2. The discussion will apply to both ratios. If there are any significant differences between the two ratios, the discussion will be separately applied to each ratio. In the following discussion, the reference to time is same as saying that it is dimensionless time, t^*.

The slider is uniformly accelerated from rest when the time is zero. When a time of 1.0 is reached, the slider assumes a uniform velocity of 1.0. During the acceleration of the slider, there is a sharp temperature rise close to the moving slider surface. This is clearly seen in the plots for $x^* = 0.1, 0.4, 0.7$ at times $t^* = 0.5$ and 1.0 (Figs. 3 - 5, 7 - 9). The high temperatures near the moving surface are due to viscous effects. At a time of $t^* = 0.5$, viscous effects have weakly penetrated across (ie. from the slider to the stationary surface) the bearing. However, the resultant velocity profiles, as seen in Figs. 11 - 13 and 15 - 17, show that the velocity of fluid closer to the slider is more fully developed than fluid adjacent to the stationary surface (or pad). Therefore, the highest shear stress occurs at the slider

surface. This is the case as shown in the plots of shear stress across the bearing (Figs. 19 - 21, 23 - 25). Thus, the highest temperatures will be located near the moving surface. At the next time interval ($t^* = 1.0$), viscous effects have strongly penetrated throughout the bearing. This is easily verified by observing that the velocity profiles at this time are not too different from the steady-state profiles (Figs. 11 - 18). The temperature profiles still exhibit sharp temperature gradients close to the slider. This is due to the fact that the slider is still being uniformly accelerated. Fluid particles in the bearing do not have a chance to catch-up to the steady-state conditions. The temperature profiles at the exit ($x^* = 1.0$) are quite different from the other upstream profiles. This is due to the effect of pressure on the development of velocities in that region. The pressure increases from zero gauge pressure at the entrance and reaches a maximum in the bearing. After that point, the pressure decreases back to zero gauge pressure at the exit. Pressure distributions are shown in Figs. 27 and 28. Velocity profiles located slightly after the point of zero pressure gradient and earlier are adversely affected by the pressures present. This causes the velocity profile to assume a bulge in the direction of flow. At a point approximately 0.1 units beyond the zero pressure gradient, the velocity profile varies linearly across the bearing.

An analysis of the full momentum equation (1) will give the reason for stating that the velocity is linear at a point beyond the zero pressure gradient. If it is assumed that steady-state is almost reached, the first term on the left-hand-side is very small compared to the other terms. Inertia terms will remain on the left-hand-side of the equals sign and pressure gradient and viscous terms on the right-hand-side. In order to get a linear velocity profile, the pressure gradient must balance the inertia terms. Therefore, a slightly negative pressure gradient is necessary to eliminate the inertia terms. When the inertia terms are neglected, the case of zero pressure gradient gives a linear velocity profile. Beyond that location, the pressure favourably affects the velocity profiles. They acquire a bulge in the direction of flow. Shear stresses are initially highest at the moving surface (Figs. 19 - 21, 23, 24). When the velocity is linear, shear stress is the same across the bearing. This can be seen in the velocity (Fig. 17) and shear stress (Fig. 25) distributions at $x^* = 0.7$ for a bearing ratio of 1.5. After that position, the highest shear stress drifts to the stationary pad (Figs. 22, 23). Therefore, heat generation will be the highest at the stationary surface. However, the bulge in the exit velocity profiles do not appear until $t^* = 1.0$.

When the time is 0.5, the shear stress at the exit (Figs. 22, 26) is almost uniformly distributed across the

top half of the bearing. Hence, heat generation is about the same across the upper half of the bearing but increases in the lower half and reaches a maximum at the slider. There is a slight bulge in the temperature profile near the moving surface (Figs. 6, 10). The profile gradually tapers off to the constant temperature boundary condition at the stationary pad. At the next time of 1.0, a second bulge in the temperature profile can be seen near the stationary pad. There is a definite shift of maximum shear stress from the slider to the stationary surface (Fig 22, 26). This shift is reflected in the temperature plots of both bearing ratios. The presence of two local temperature maxima at this time could be explained in the following manner. Initially, shear stresses, from the entrance to the point of linear velocity, are the highest on the moving surface (Figs. 19 - 21, 23 - 25). As a result, the highest temperatures are developed near that surface. When the maximum shear stress shifts to the stationary surface, the highest heat generation is now located on this surface (Figs. 22, 26). Therefore, local temperature peaks start to form near the stationary surface. In other words, the development of temperature peaks at the stationary surface occurred in the latter part of the bearing. When the time is 1.5, the two ratios are discussed individually.

For a bearing ratio of 2.2, the shear stresses in the bearing correspond closely to the location of maximum

temperatures. The temperature profiles at $x^* = 0.1$, 0.4 and 0.7 have maximums which correspond well with the location of maximum shear stress (Figs. 3 - 5, 19 - 21). The highest shear stress at these locations are at the moving surface. At the exit, the correspondence does not hold for this ratio (Figs. 6, 22). Instead, the highest temperatures are near the slider and maximum shear stress is at the stationary pad. The higher shear stresses at the pad result in higher heat generation but the overall temperature increase is not great enough to exceed the temperatures at the slider. When a comparison is made between the graphs at $x^* = 0.7$ and 1.0 (Figs. 5, 6), it can be seen that the temperature rise near the pad is 0.04 (12.5°C) and at the moving surface is 0.016 (5.0°C). However, the temperatures near the slider still remain higher than the temperatures near the pad.

For a bearing ratio of 1.5, the location of maximum shear stress roughly corresponds to the location of maximum temperatures. At $x^* = 0.1$ and 0.4, the temperatures across 80% of the bearing are about the same (Figs. 7, 8) but the highest shear stresses are at the slider (Figs. 23, 24). The shear stress at $x^* = 0.7$ is approximately the same across the bearing (Fig. 25). This is expected because the location of linear velocity (Fig. 17) is about 0.1 units from the point of zero pressure gradient (at 0.6) as seen in the pressure distribution graph

(Fig. 28). The temperature at this point is a maximum near the pad (Fig. 9). At the exit, heat generation is higher at the pad than at the slider (Fig. 26). The temperature increase from $x^* = 0.7$ to 1.0 is 0.04 (12.5°C) near the pad and 0.018 (5.6°C) near the slider. It is interesting to note that the increases in this region are about the same for both ratios. However, the temperature increase near the slider is slightly higher for K = 1.5.

When a comparison is made between corresponding shear stress profiles for the two bearing ratios (compare Figs. 19 - 22 with Figs. 23 - 26), it is apparent that the overall shear stress in the bearing with the smaller ratio is higher than the larger ratio. This means that the heat generated in the former bearing is higher and will result in higher temperatures. This is the case when temperature profiles at the same location are compared (compare Figs. 3 - 6 with Figs. 7 - 10). The highest temperatures for both bearing ratios occur at the exit (Figs. 6, 10). For a ratio of 2.2, the highest temperature is 1.0815 (65.5°C) and, for a ratio of 1.5, the highest temperature is 1.12 (77.6°C). The surface temperatures were assumed to be at 40°C. Therefore, the maximum temperature rise for the higher and lower bearing ratios are 25.5°C and 37.6°C, respectively. According to ref.[11,12], a temperature rise of approximately 30°C should not be exceeded. However, any substantial deviation from this value will affect bearing

performance. Therefore, the higher ratio bearing has an acceptable temperature rise. The temperature rise in the the other bearing is about 25% above the accepted value. This is not too great a deviation from the norm. For the lower ratio bearing, the flatness in the profiles could be due to a combination of high heat generation and the resulting increase in heat conduction across the bearing. The earlier shift in maximum temperature, from the slider to the pad, for the bearing ratio of 1.5 is due to the change in favourable pressure gradient at $x^* = 0.6$ instead of $x^* = 0.7$ for the other ratio (Figs. 5, 9). Since the temperatures in the bearing were already quite evenly distributed, a change in maximum shear stress is quickly reflected in the temperature profiles.

With reference to the velocity and shear stress, it is seen that the profiles from a time of 1.5 to steady-state form a single curve (Figs. 11 - 26). It would seem that steady-state has been reached at a time of 1.5. However, the temperature fields indicate that steady-state has not been reached even at a time of 3.0 (Figs. 3 - 10). Actually, there are differences in the velocity curves for times greater than 1.5 but the differences between the values are not significant enough to be evident in the graphs. This is also the case for the shear stress curves. But these small differences are greatly amplified in the temperature graphs. The largest differences occur at the

exit because smaller differences upstream tend to have an additive effect on subsequent downstream temperatures. Therefore, it can be surmised that transient velocities and shear stresses reach the steady-state condition faster than transient temperatures. There is a greater temperature difference in the thrust bearing with ratio of 1.5 than the one with a 2.2 ratio. The differences between transient ($t^* = 3.0$) and steady-state temperatures are less than 5%. This is generally the case for most of the profiles except for the profiles at the exit where the difference is less than 10%. For the velocity and shear stress distributions, the differences between the transient and steady-state values is insignificant after $t^* = 1.5$.

Therefore, it can be concluded that steady-state conditions exist for the velocity and shear stress distributions when a time of 1.5 is reached. This assumption is not valid for temperature profiles at that time. However, the profiles at a time of 3.0 adequately represent steady-state conditions. The differences could be further reduced by carrying out computations for a longer time period but, the changes between succeeding temperature values decreases as time increases. Therefore, there will not be much improvement for computations beyond a time of 3.0. However, the costs will still continue to increase at a constant rate. The law of diminishing returns made it necessary to terminate computations at a time of 3.0.

Transient temperature profiles for the case of an adiabatic slider

A comparison between the temperature distributions for an adiabatic slider and a constant temperature slider shows that the only significant differences occur close to the slider (Figs. 3 - 10 and 29 - 36). The curves follow very similar paths at distances greater than 0.3 units away from the slider. The high temperatures at the slider surface are the result of no heat conduction through the slider. Therefore, any heat generated at that surface can only be conducted into the fluid. When a surface is adiabatic, it is usually the case that the highest temperature will be found on that surface. However, an examination of the graphs will reveal that the maximum temperatures in the bearing occur in the fluid. The shift in maximum temperature from the adiabatic surface could be due to a combination of factors. Factors such as convection, conduction, and viscous effects could contribute to such a shift. Perhaps, an analysis of individual energy terms may throw some light on this phenomenum. It may also be possible to uncover the reason why there are two temperature maxima at the exit of the bearing with the ratio of 2.2.

The first energy terms to be analysed will be the two convective terms. The first term is concerned with convection along the bearing and the other is concerned with convection across the bearing. Initially, the first term

will be analyzed (Fig. 37). It shows that there is very high convection close to the slider surface compared to convection near the pad. This high rate persists over most of the bearing length ($x^*= 0.7$). This would mean that higher temperatures would be near the moving surface. As seen in the graphs (Figs. 29 - 31), the higher temperatures are located in the lower half of the bearing. Around $x^*= 0.8$, convection is about the same across 70% of the bearing and is lower for the remaining 30% near the pad. Therefore, the temperatures slightly above the middle of the bearing ($y^*= 0.5$) should be starting to catch-up with temperatures near the slider. This increase is partially reflected in the temperature curves at $x^*= 0.7$. At the exit, convection is very high between 0.5 and 0.7. The term reaches a value of about 0.1 units. If the temprature profiles at the exit is examined (Fig. 32), it is seen that the location of a second temperature peak also occurs in that region. Therefore, it can be concluded that the first term does help explain the overall shapes of the temperature profiles. The overall trend in the convection term has been observed in ref.[2]. In that paper, a plot of temperature gradient versus x^* was done. The general shape of the curves at the pad and slider were about the same. It is still not quite clear why the highest temperature is not located on the adiabatic surface.

Now, the other convection term (Fig. 38) will be discussed. For most of the length of the bearing, this term does not contribute much to the overall temperature picture. From the entrance to 0.7, this term does not exceed 0.025 units. It is beyond the point of linear velocity ($x^* = 0.8$) that this term begins to contribute significantly to the overall temperature profile. Convection is higher at the top 30% of the bearing. Such high convection rates help to rapidly increase temperatures near the pad. This observation was made earlier for the case of constant slider temperature. However, the contribution of both convection terms do not make the temperatures near the pad higher than temperatures near the slider.

The graph of the conduction term (Fig. 39) shows a somewhat confusing jumble of curves that have been plotted for various distances across the bearing. At the exit, it would seem that the highest conduction occurs around 0.4 and 0.5. Conduction tapers off to either side of this region. In that region, there is the presence of a saddle. To either side of the saddle, the temperatures are higher. This is seen in the temperature plot (Fig. 32).

An analysis of the viscous term (Fig. 40) shows that viscous effects across the bearing stay quite constant from $x^* = 0$ to 0.7. As expected, the highest viscous effects are close to the moving surface. Beyond the point of linear velocity (about 0.8), there is a reversal of

viscous effects. The highest viscous effects are now at the pad. At the exit, the very high viscous effects (0.22) at the pad contributed a great deal to the temperature increase in the region.

In summary, it can be said that all the energy terms contributed in some way to the overall temperature profiles. The lower temperature on the adiabatic surface could be due to numerical inaccuracies. Numerical solution of temperature at and near the moving surface is based on a less accurate finite difference formula.

CHAPTER V

CONCLUSIONS

Studies were made on a thrust bearing with two different slider boundary conditions, namely, constant temperature and adiabatic surface. A number of numerical simulations were performed using different bearing ratios and Prandtl and Eckert numbers.

For the case of a constant slider temperature, it was found that the location of highest temperatures depended on the bearing ratio. The highest temperature was located near the slider for a bearing ratio of 2.2 and near the pad for a bearing ratio of 1.5. Steady-state was reached (within 10%) at a time of 3.0.

For the case of an adiabatic slider, the temperatures on the slider were much higher than in the previously considered case. However, the overall temperature profiles, except close to the adiabatic surface, are not too different from the other case. If the temperature at the surface is too high, cooling is required. Hence, this case would indicate whether a constant temperature slider is needed.

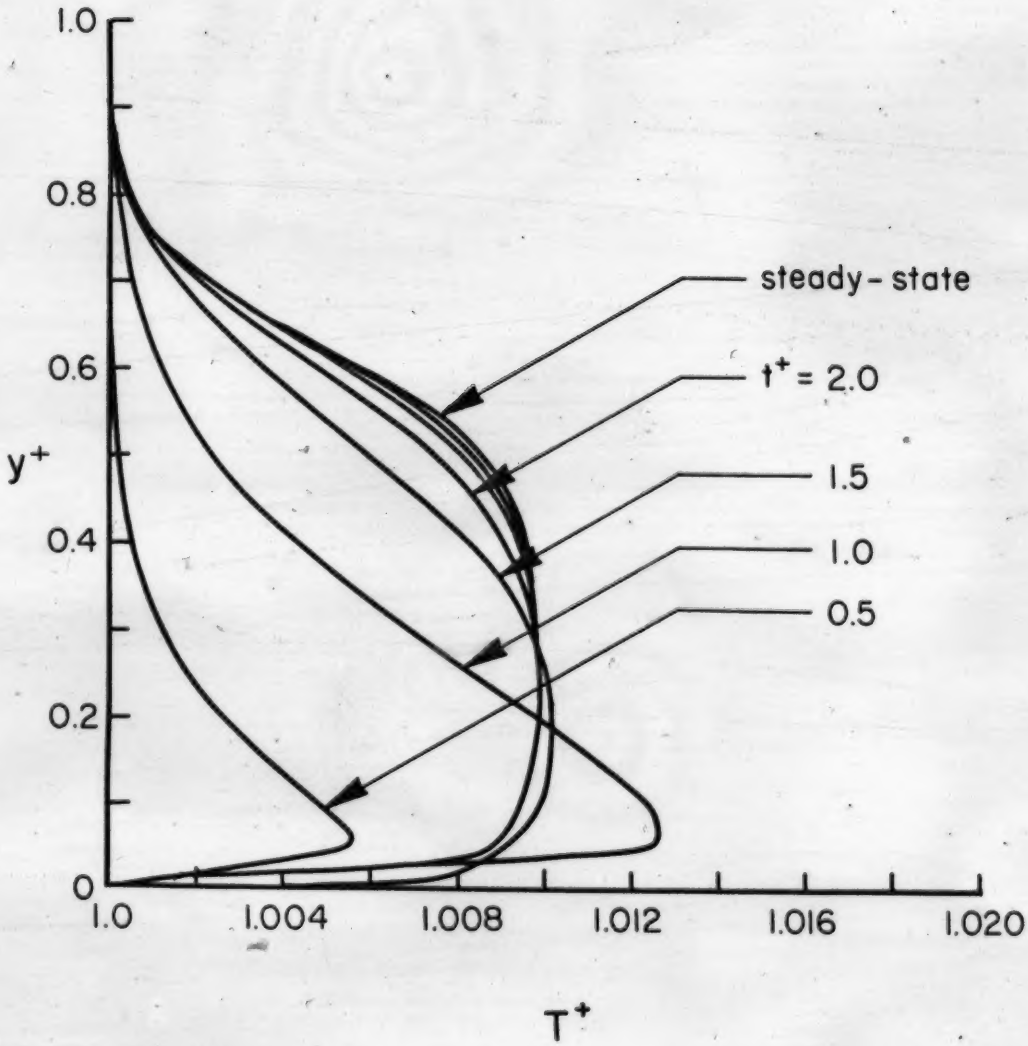

Fig. 3. Transient temperature distribution at $x^+ = 0.1$ for $K = 2.2$ (constant slider temperature)

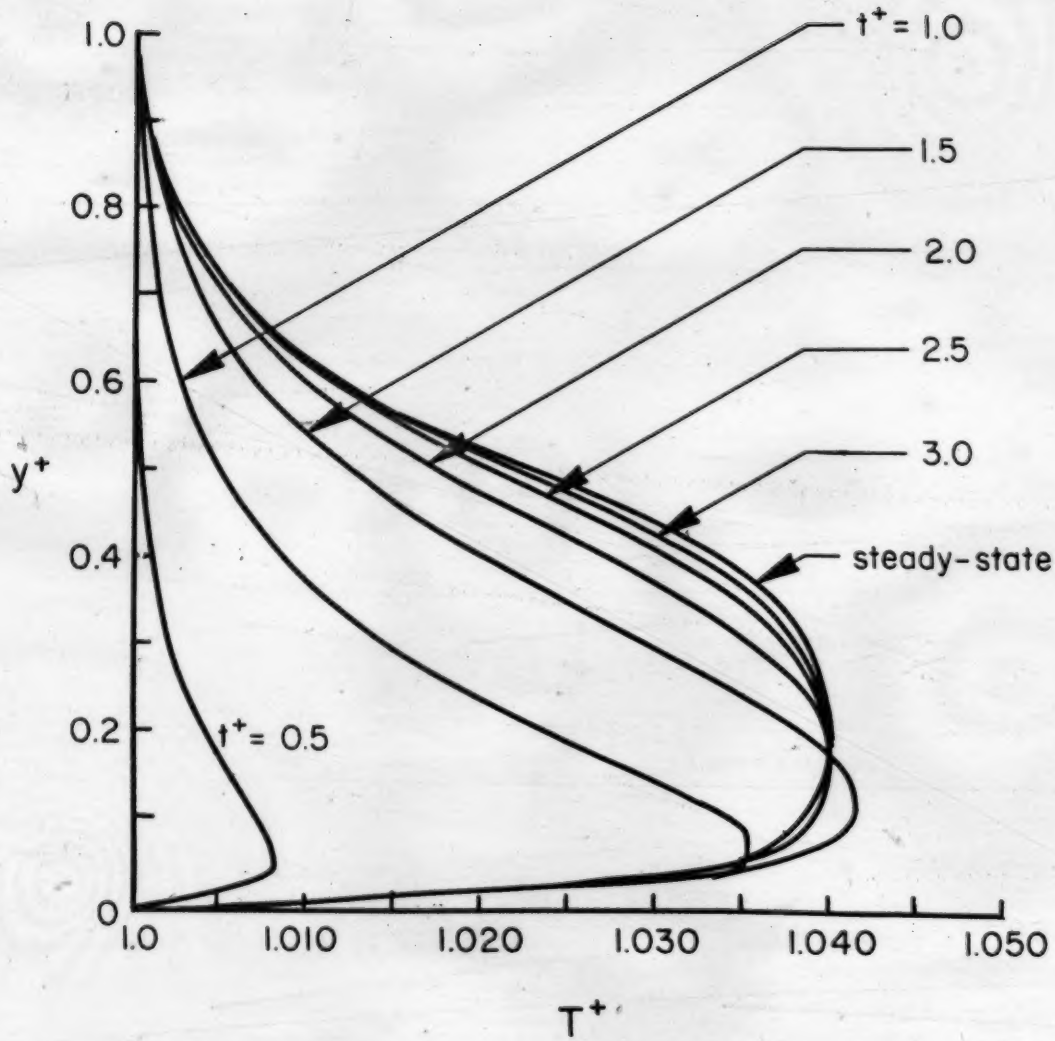

Fig. 4. Transient temperature distribution at $x^* = 0.4$ for $K = 2.2$ (constant slider temperature)

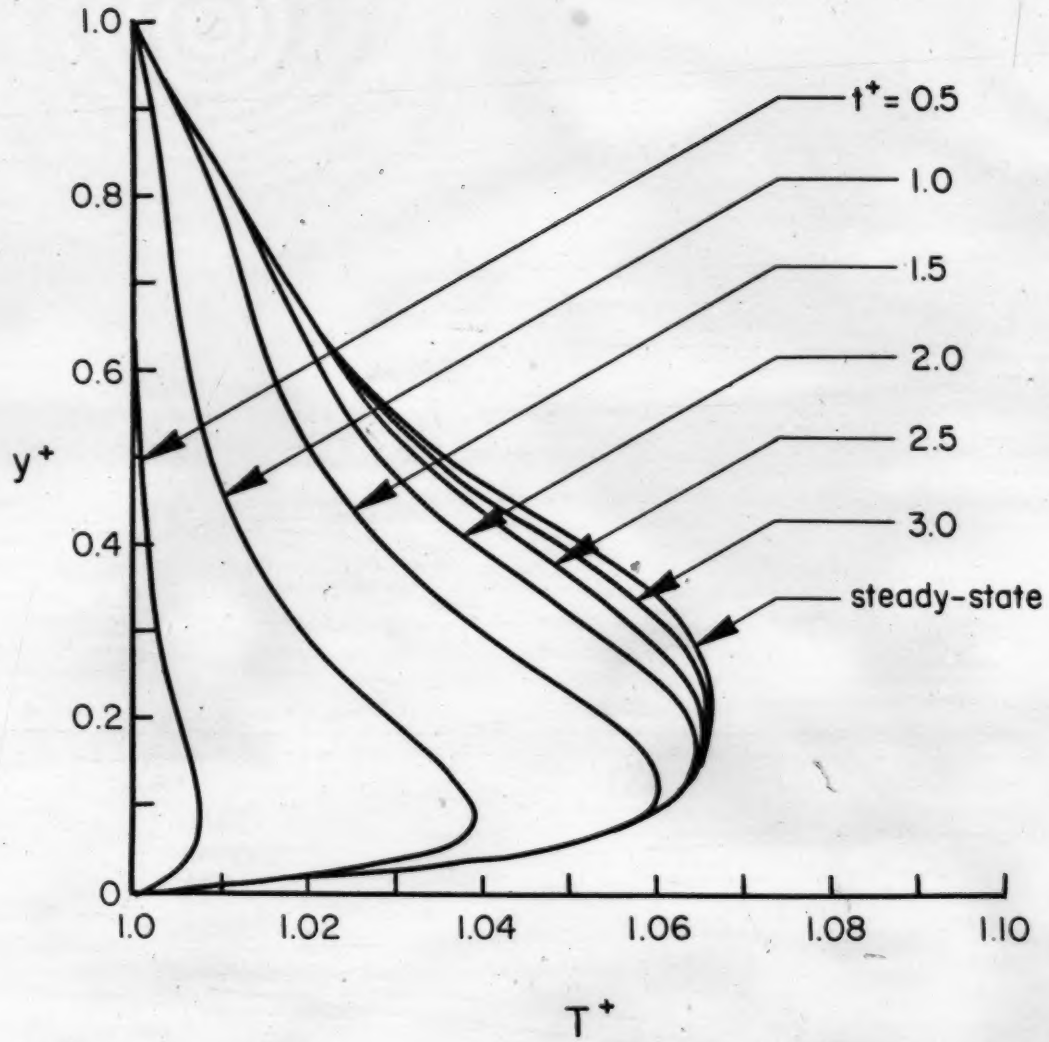

Fig. 5. Transient temperature distribution at $x^+ = 0.7$ for $K = 2.2$ (constant slider temperature)

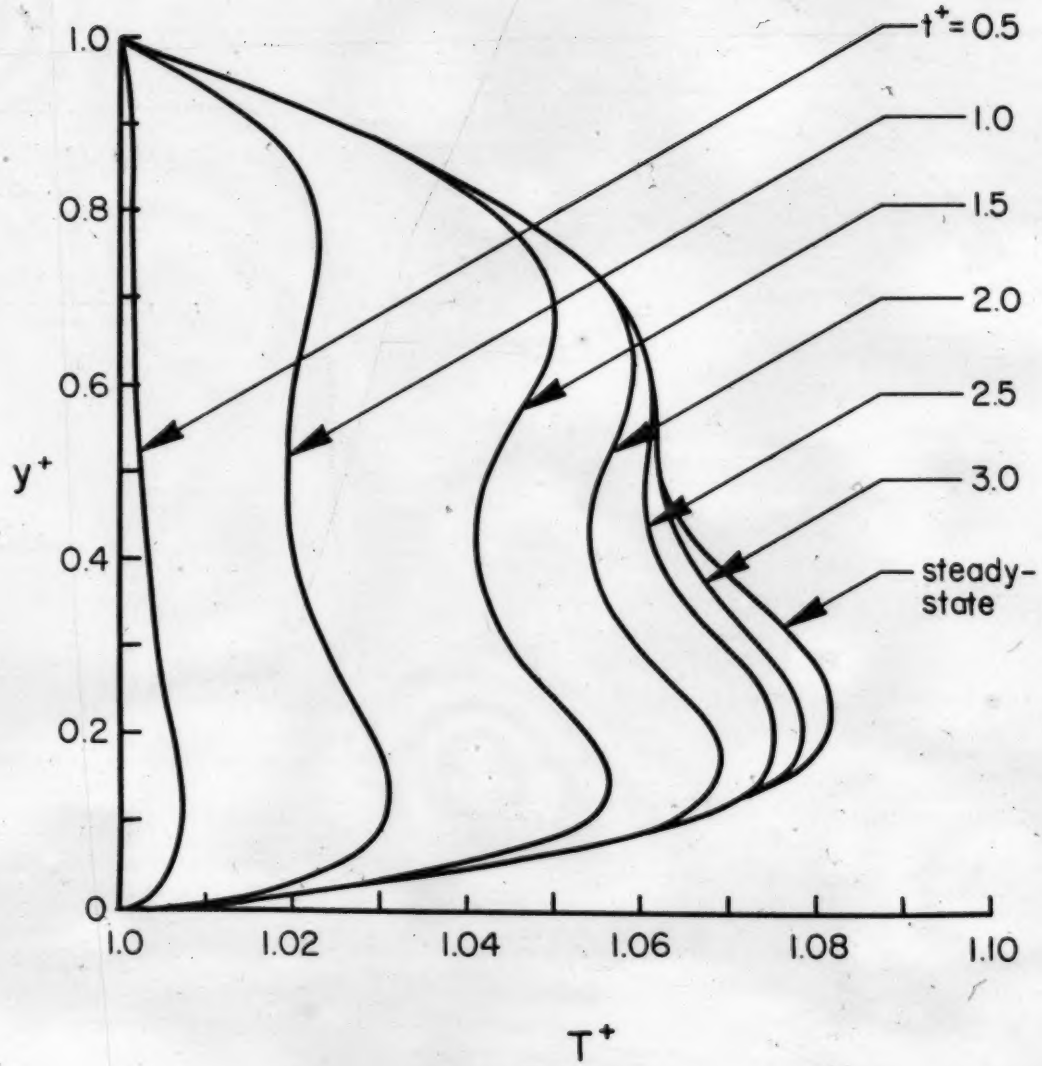

Fig. 6. Transient temperature distribution at $x^+ = 1.0$ for $K = 2.2$ (constant slider temperature)

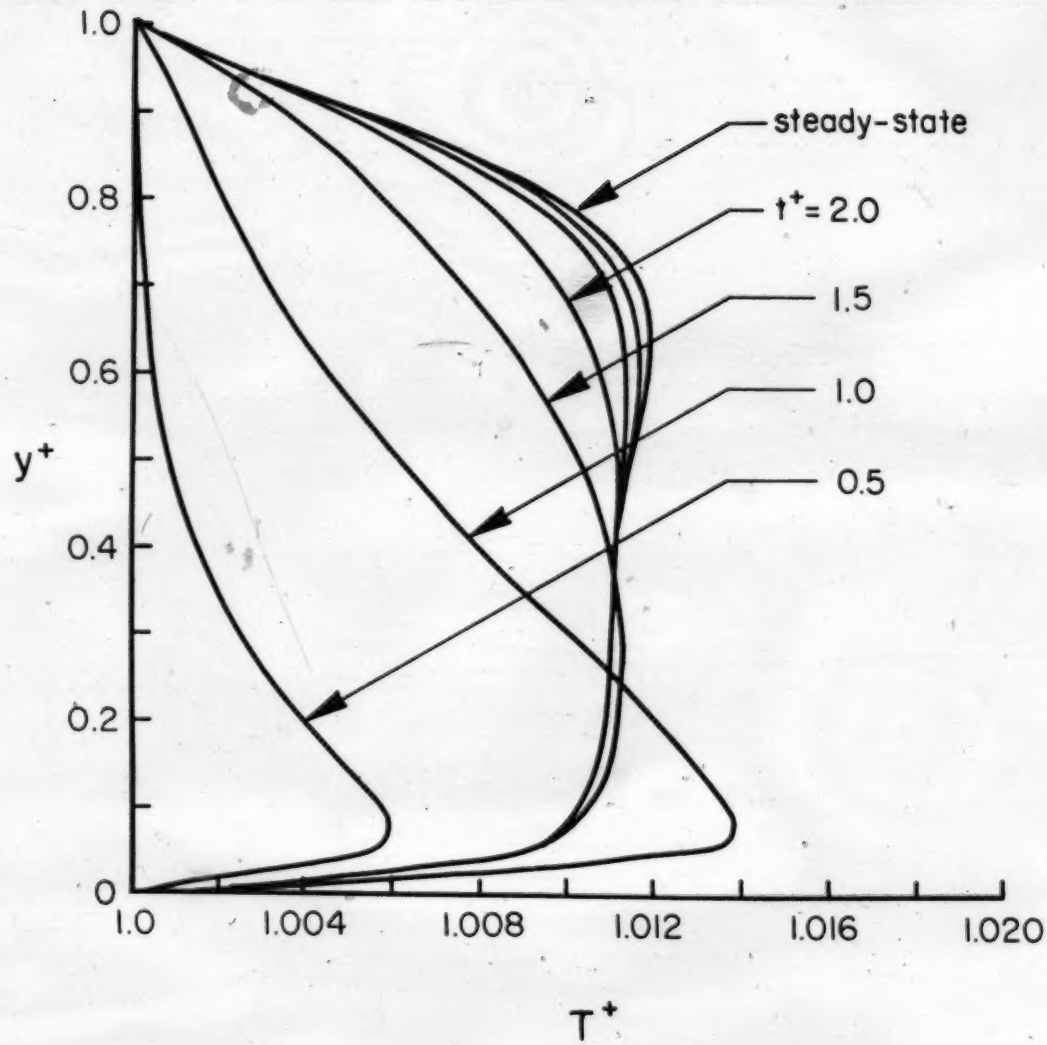

Fig. 7. Transient temperature distribution at $x^+ = 0.1$ for $K = 1.5$ (constant slider temperature)

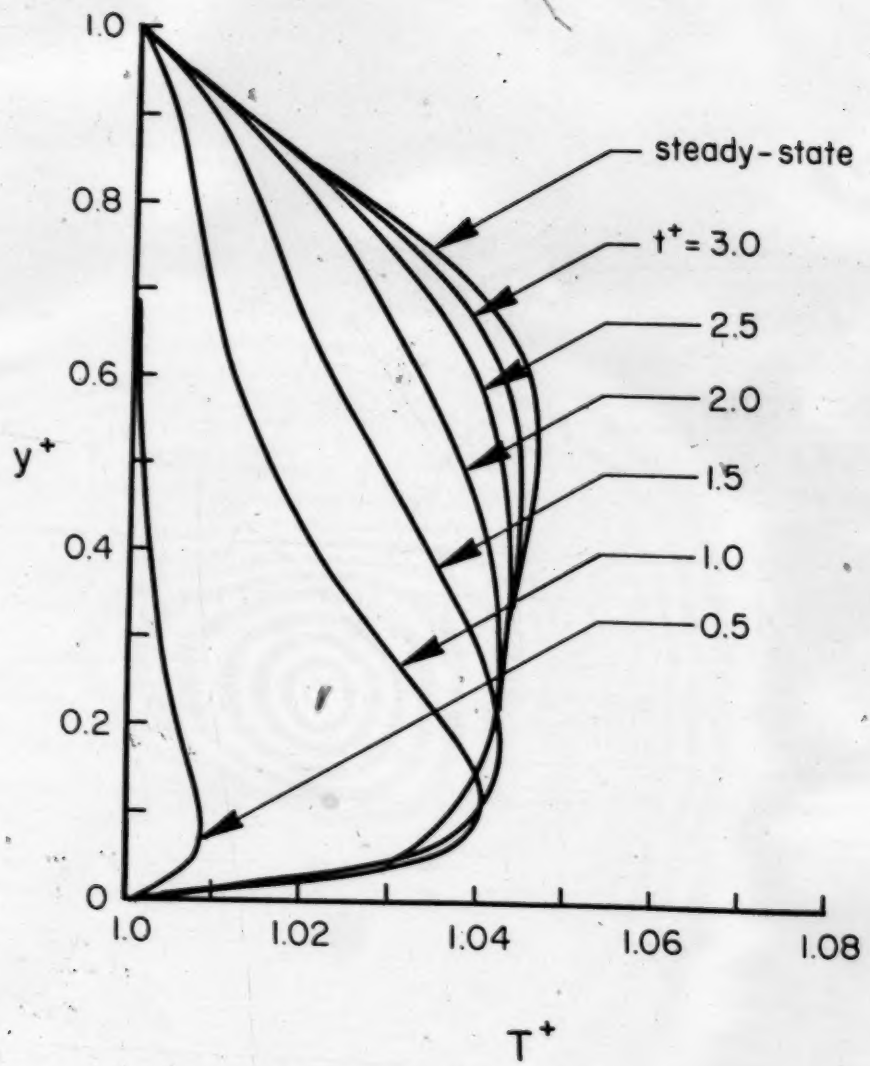

Fig. 8. Transient temperature distribution at $x^+ = 0.4$ for $K = 1.5$ (constant slider temperature)

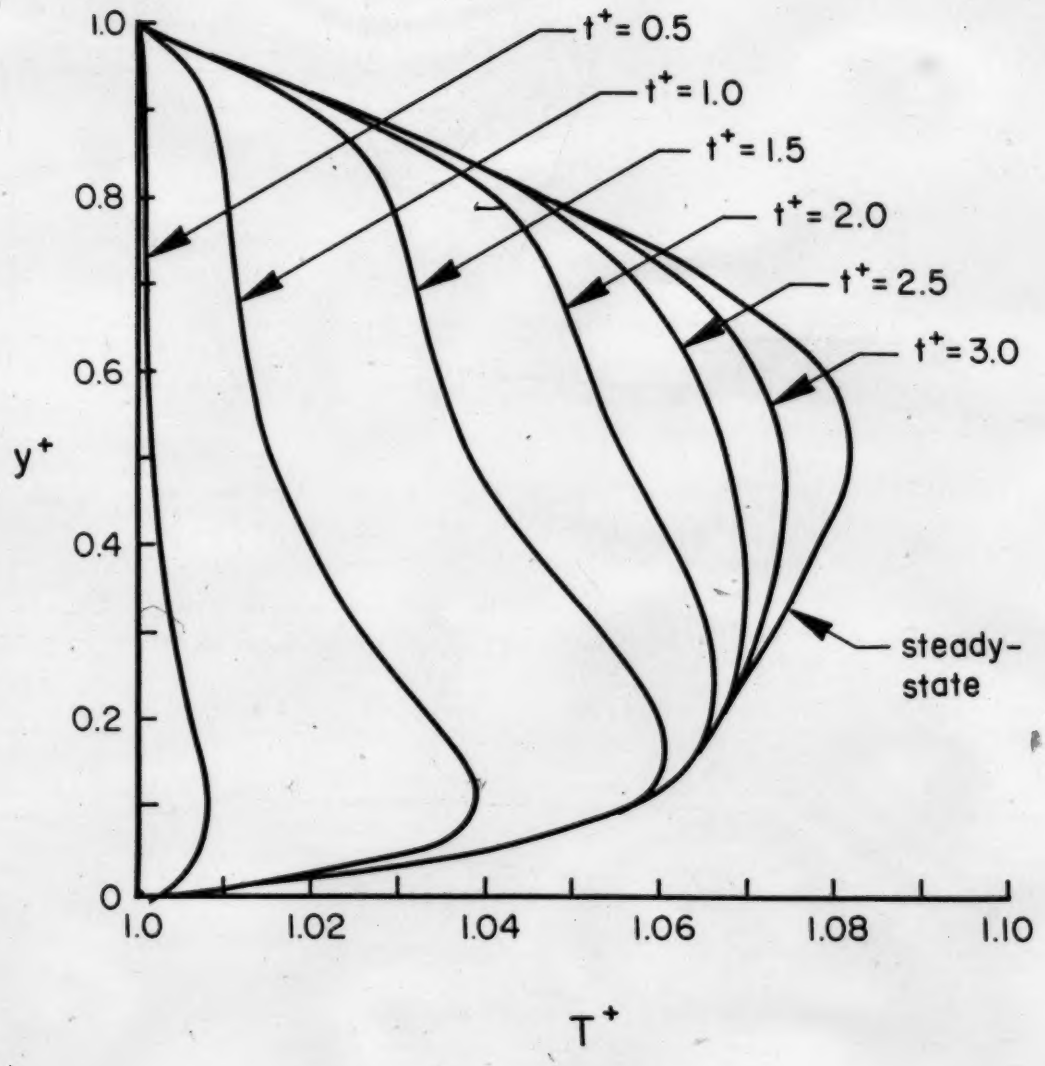

Fig. 9. Transient temperature distribution at $x^+ = 0.7$ for $K = 1.5$ (constant slider temperature)

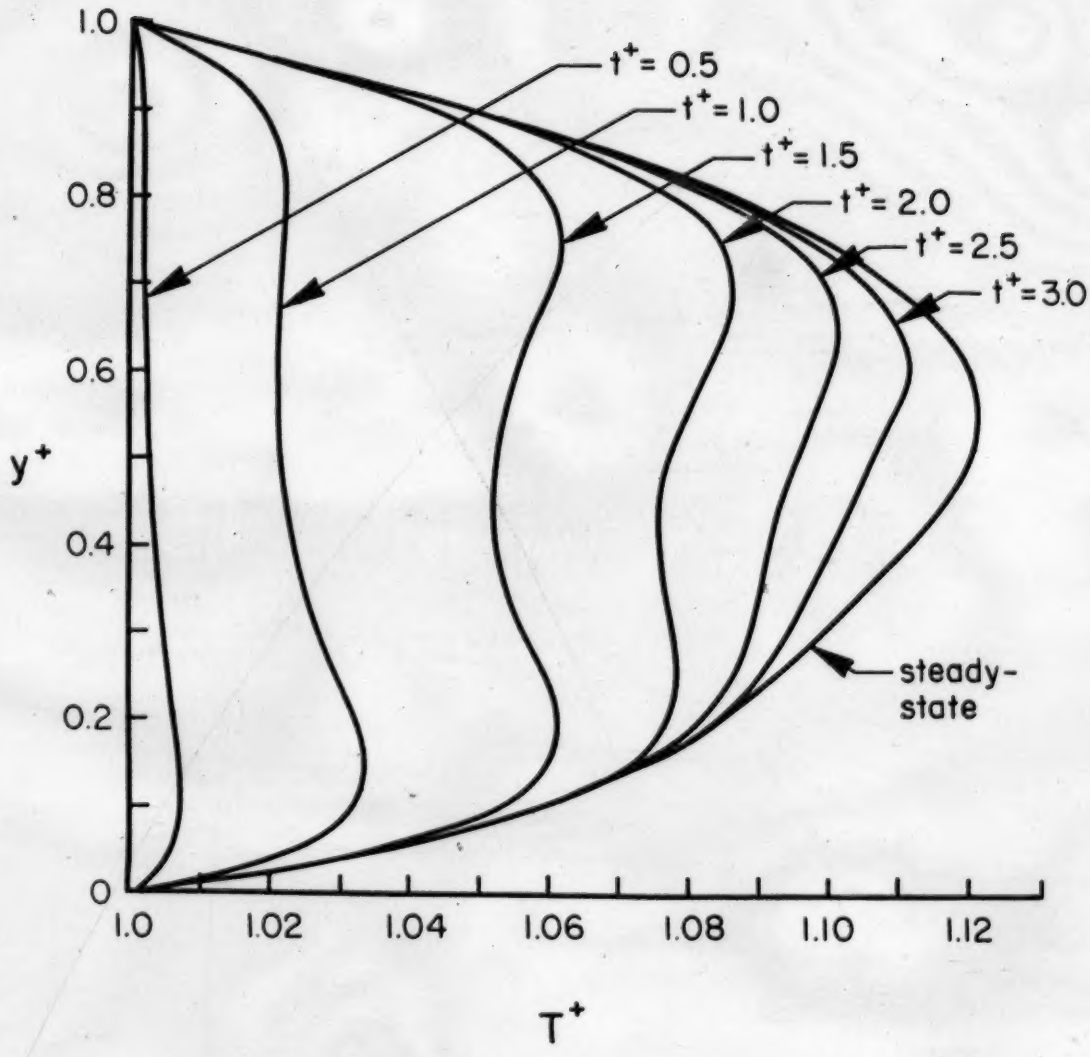

Fig. 10. Transient temperature distribution at x'= 1.0 for K = 1.5 (constant slider temperature)

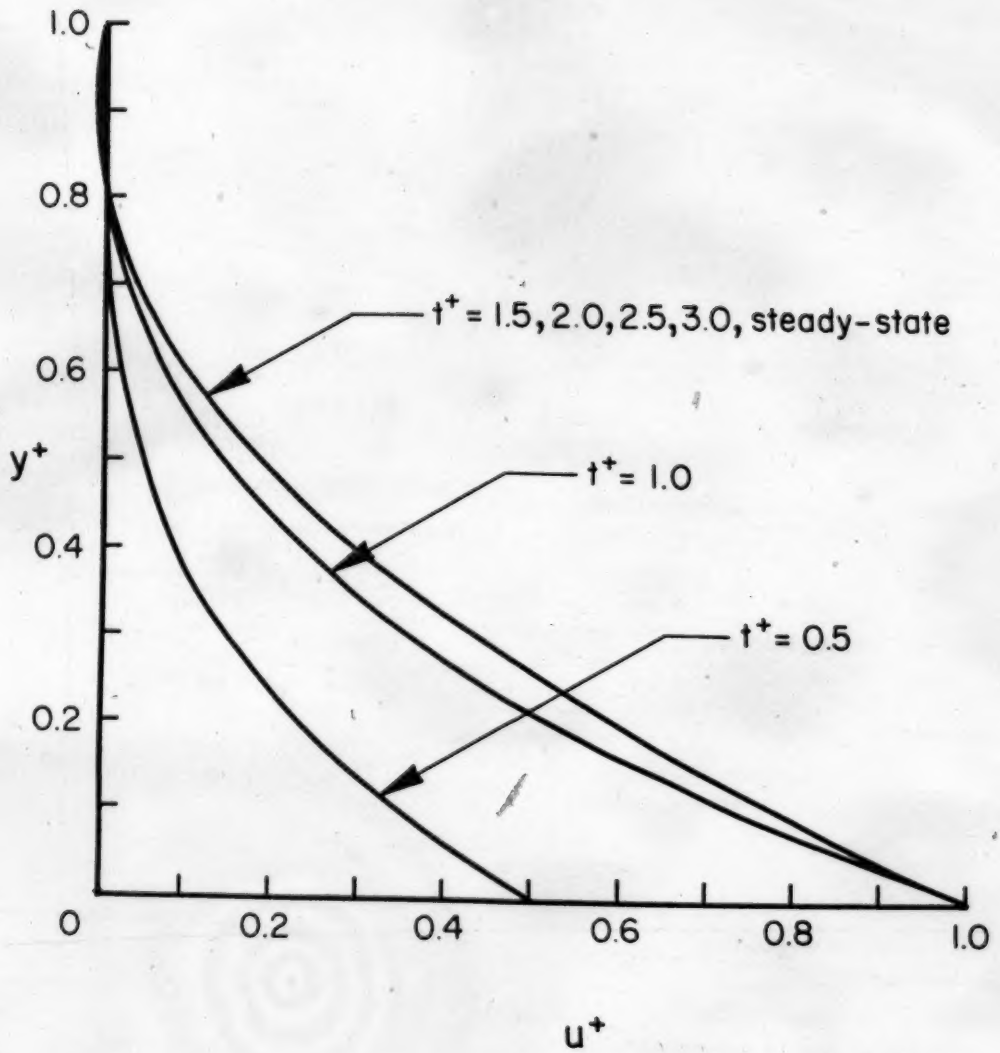

Fig. 11. Transient velocity distribution at x* = 0.1 for K = 2.2

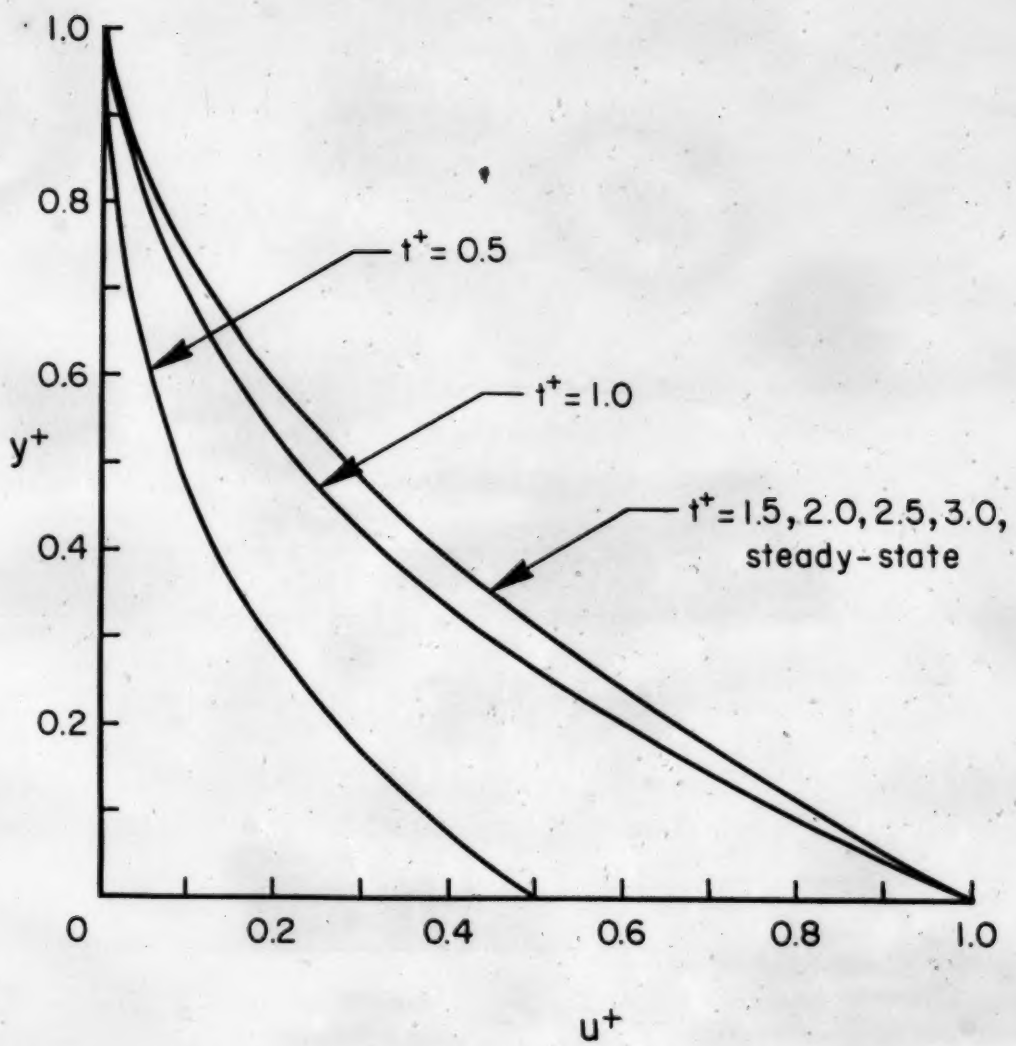

Fig. 12. Transient velocity distribution at $x^+ = 0.4$ for $K = 2.2$

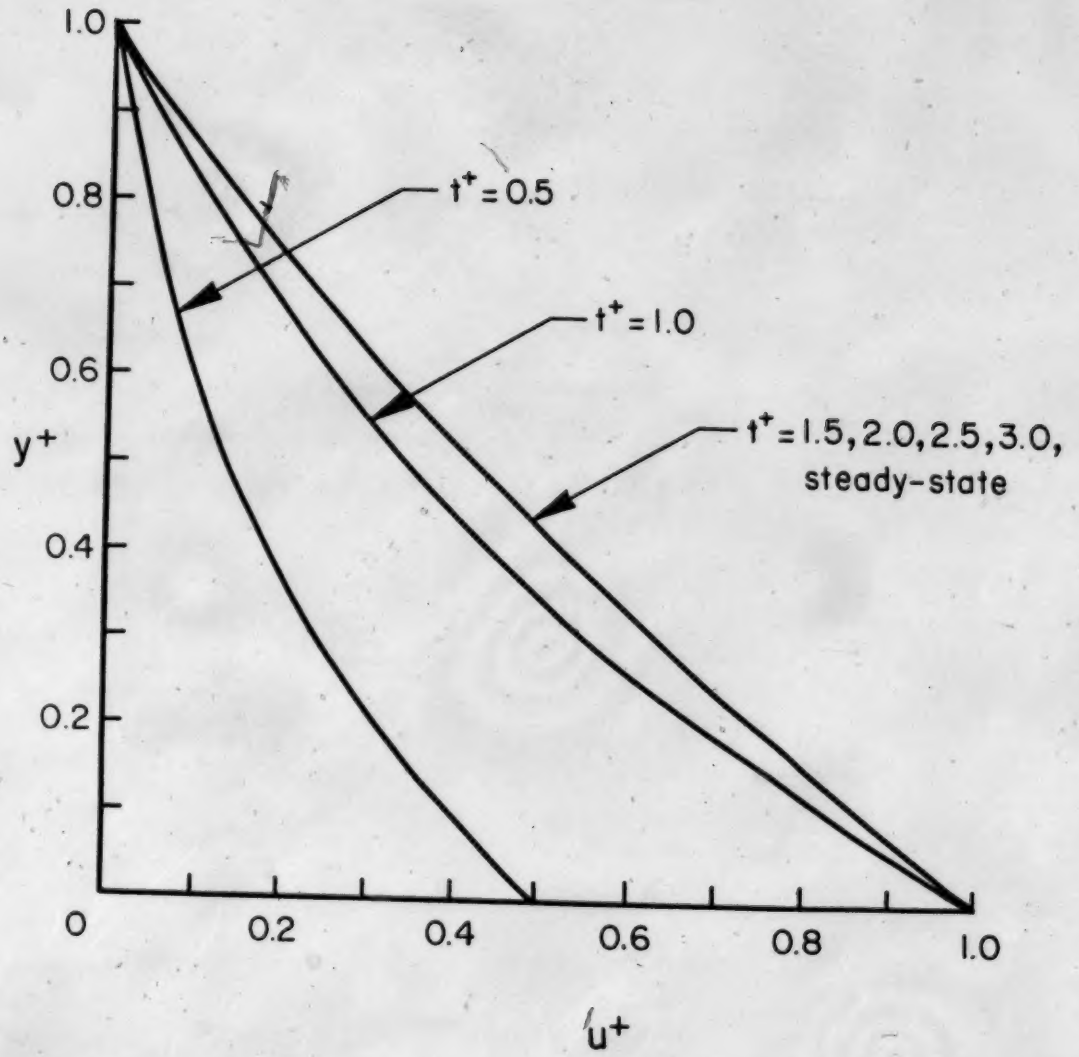

Fig. 13. Transient velocity distribution at x' = 0.7 for K = 2.2

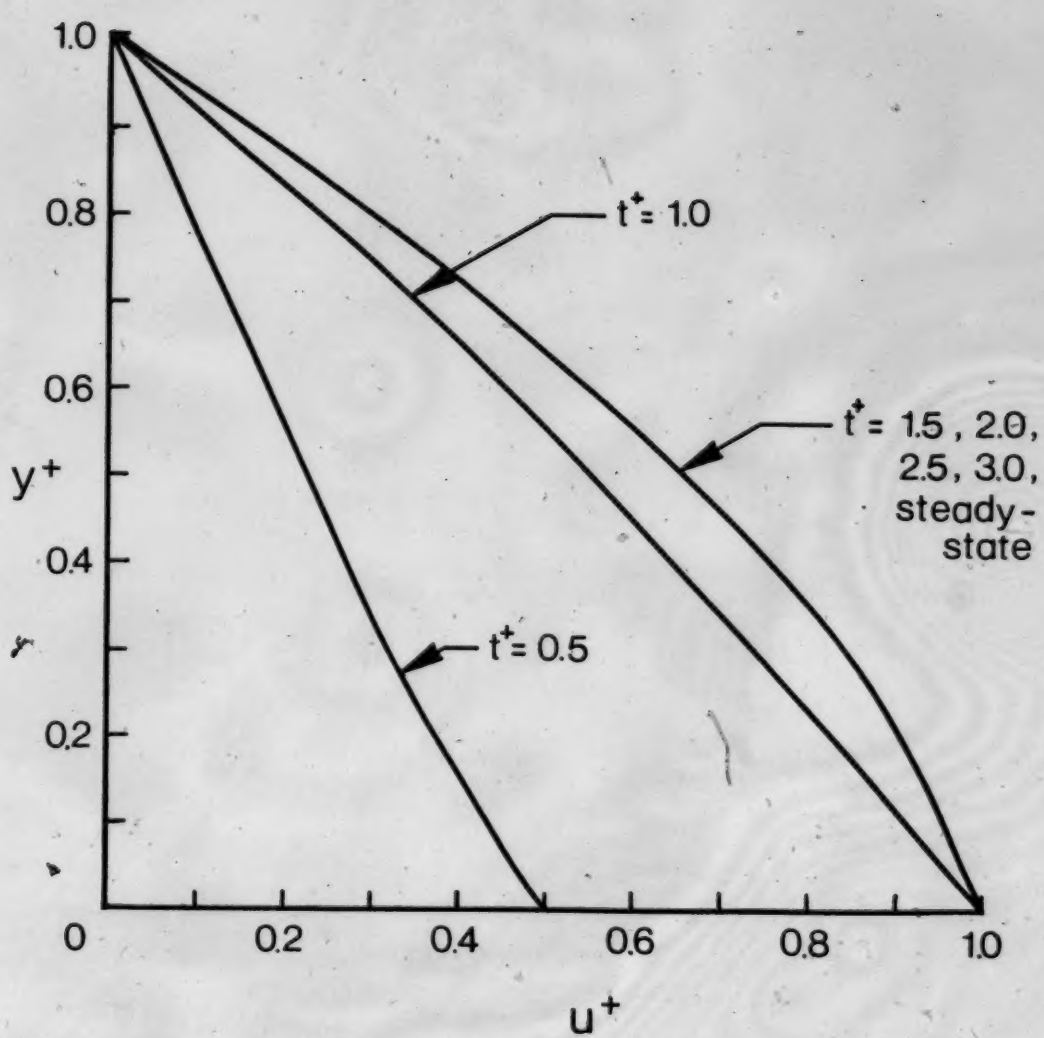

Fig. 14. Transient velocity distribution at $x^+ = 1.0$ for $K = 2.2$

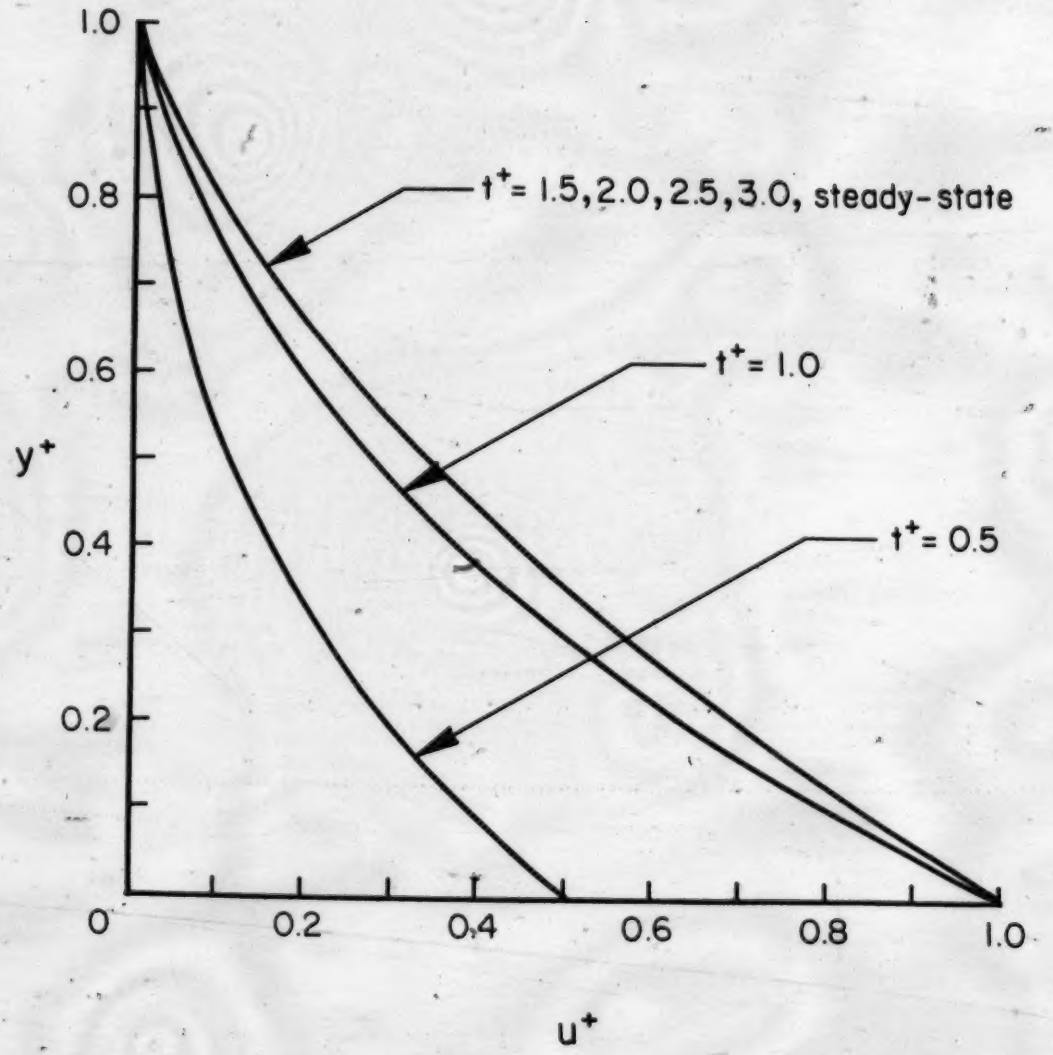

Fig. 15. Transient velocity distribution at x'= 0.1 for K = 1.5

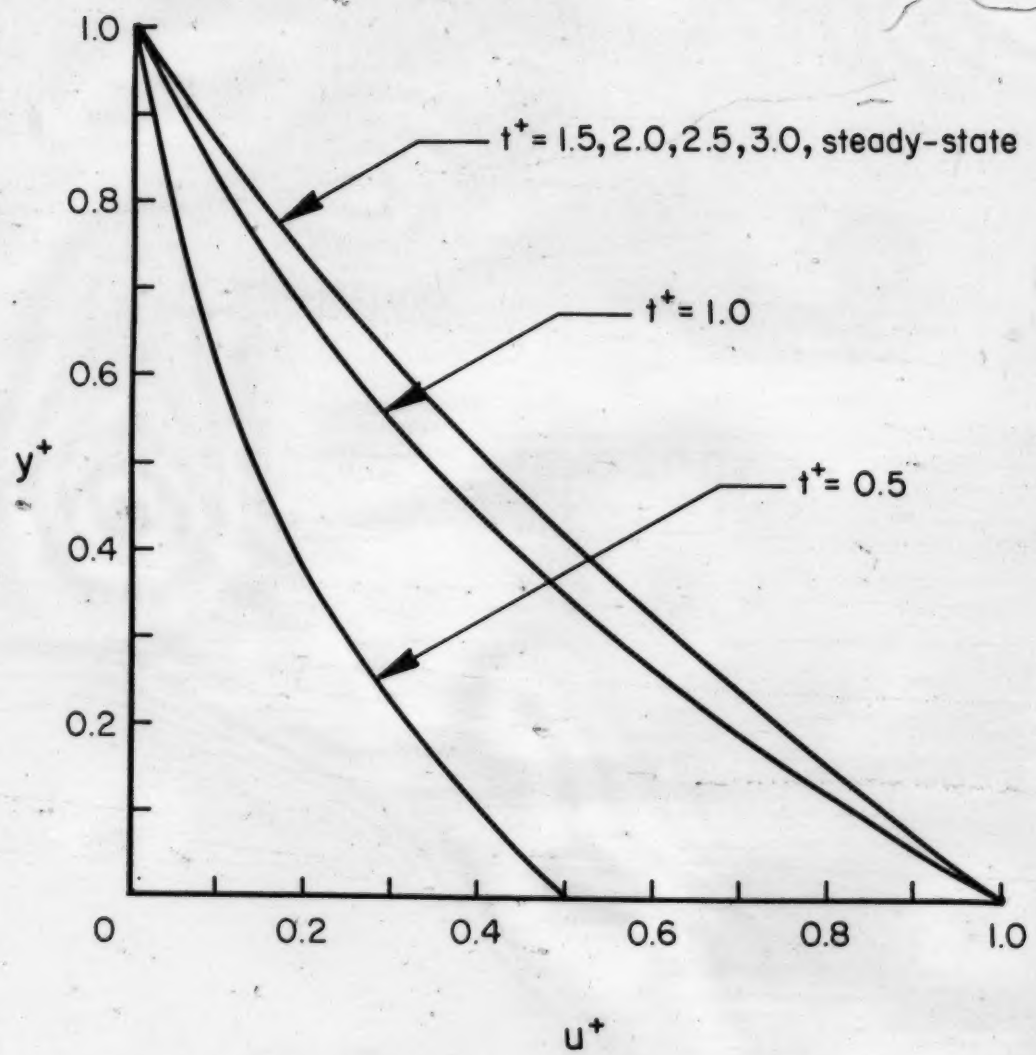

Fig. 16. Transient velocity distribution at $x^+ = 0.4$ for $K = 1.5$

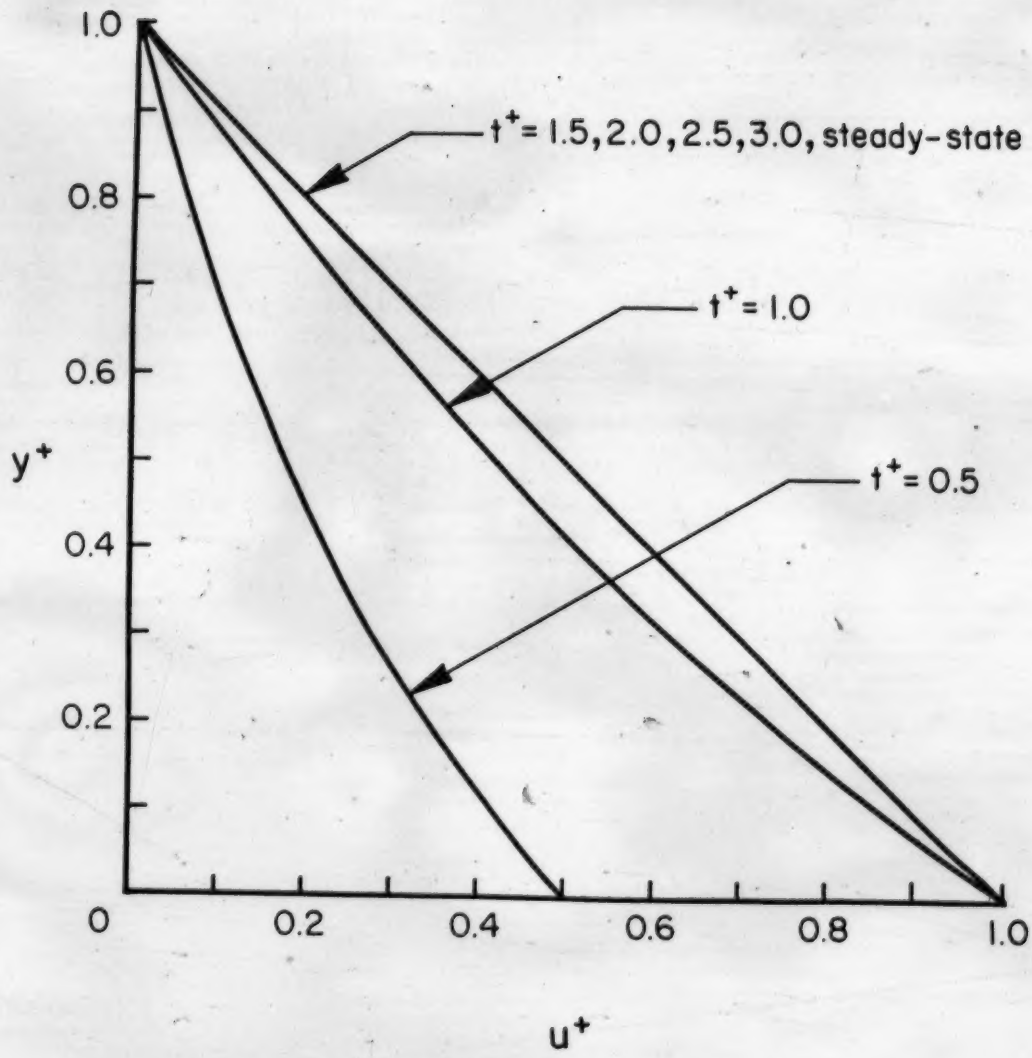

Fig. 17. Transient velocity distribution at x'= 0.7 for K = 1.5

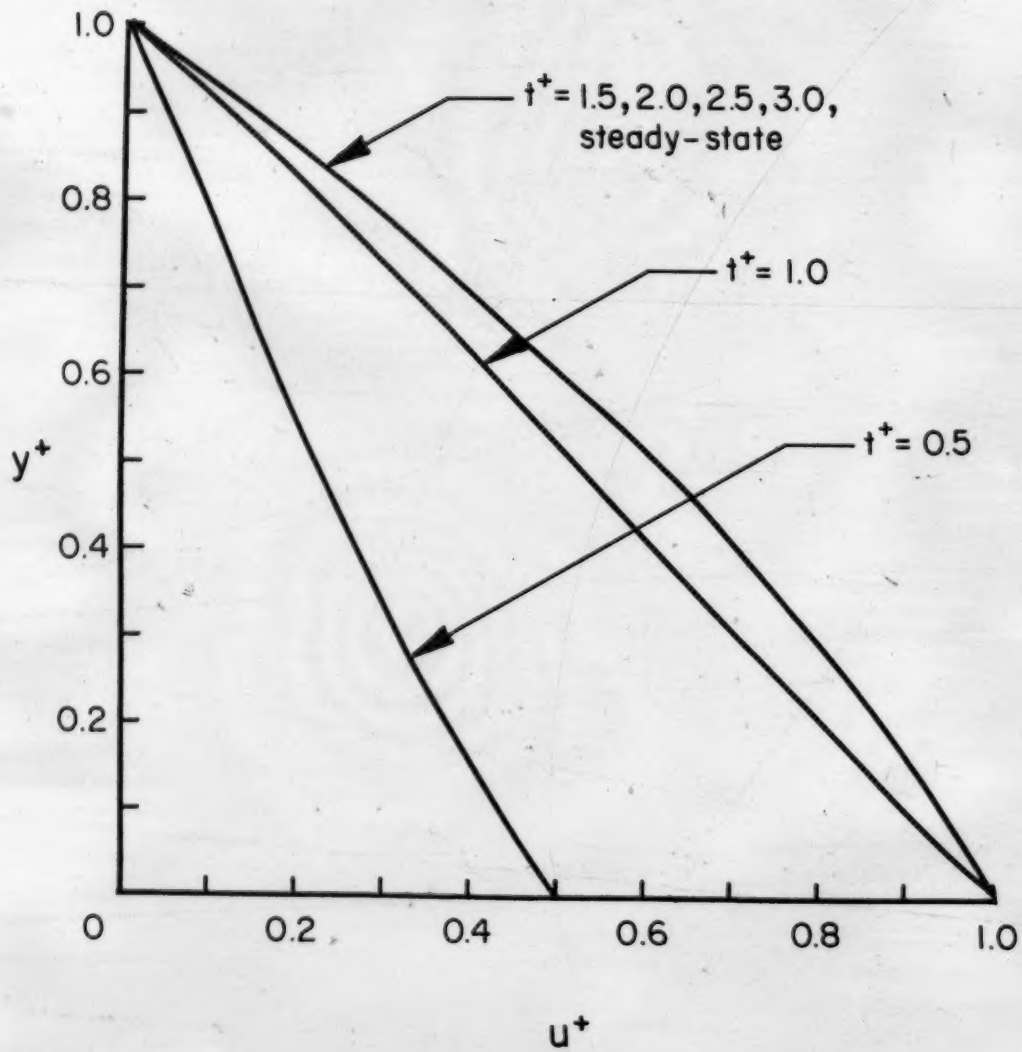

Fig. 18. Transient velocity distribution at x'= 1.0 for K = 1.5

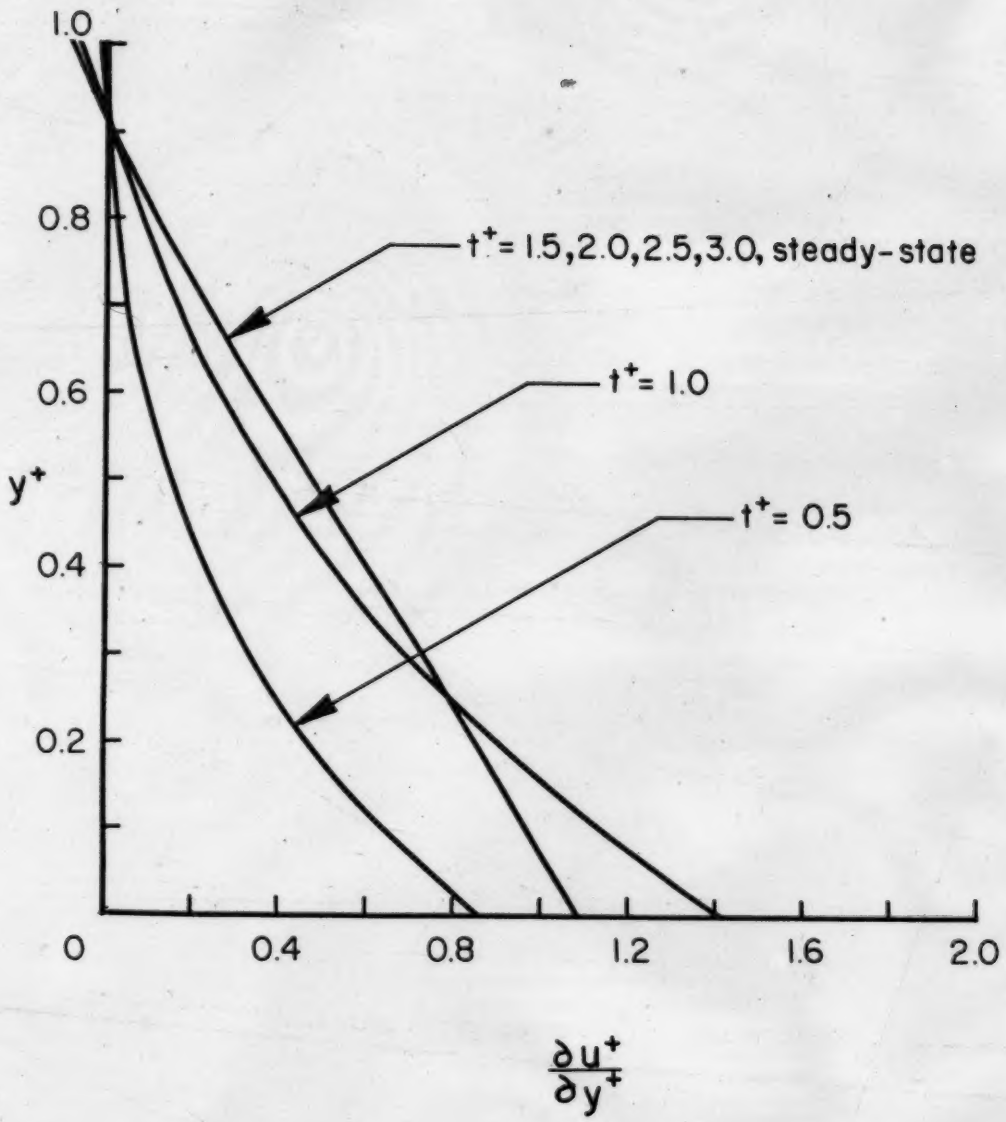

Fig. 19. Transient shear stress distribution at x'= 0.1 for K = 2.2

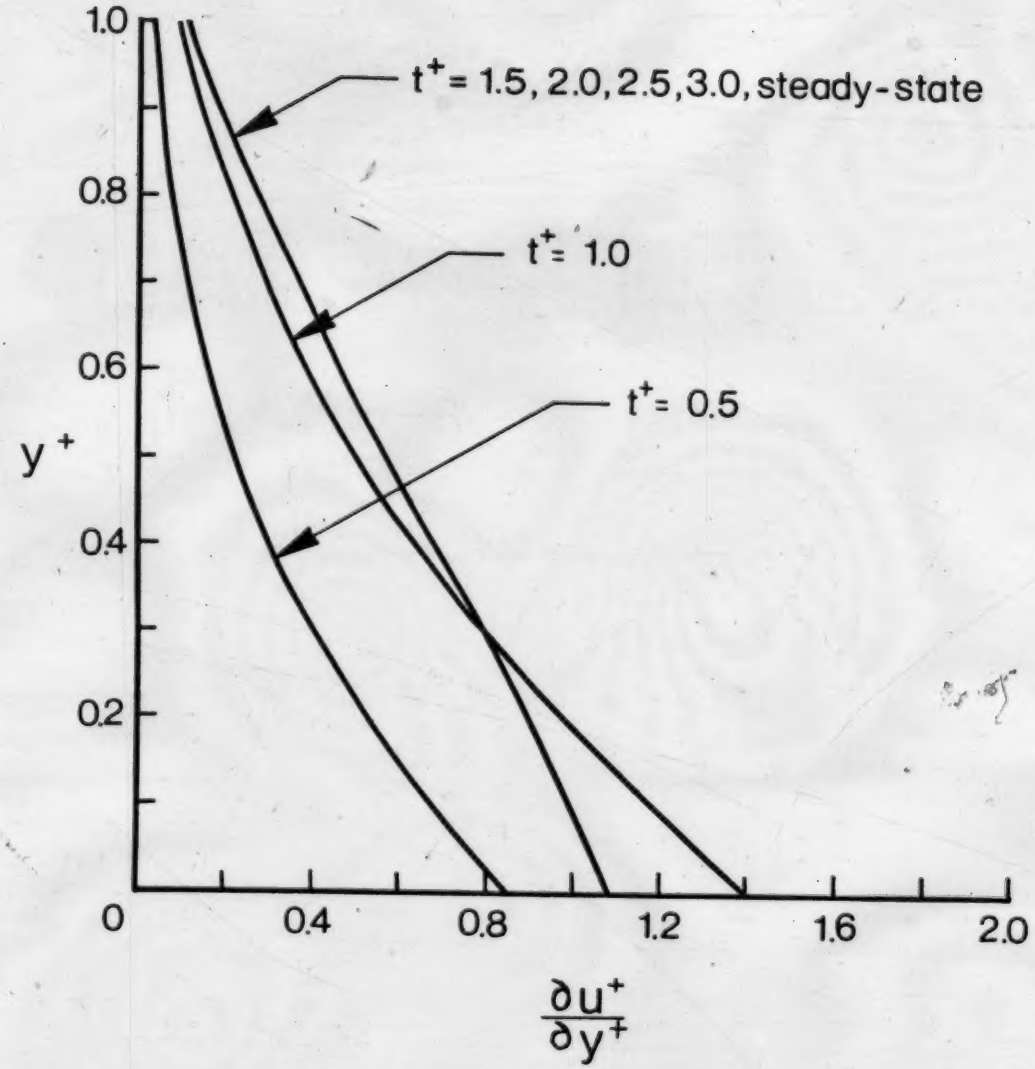

Fig. 20. Transient shear stress distribution at x+= 0.4 for K = 2.2

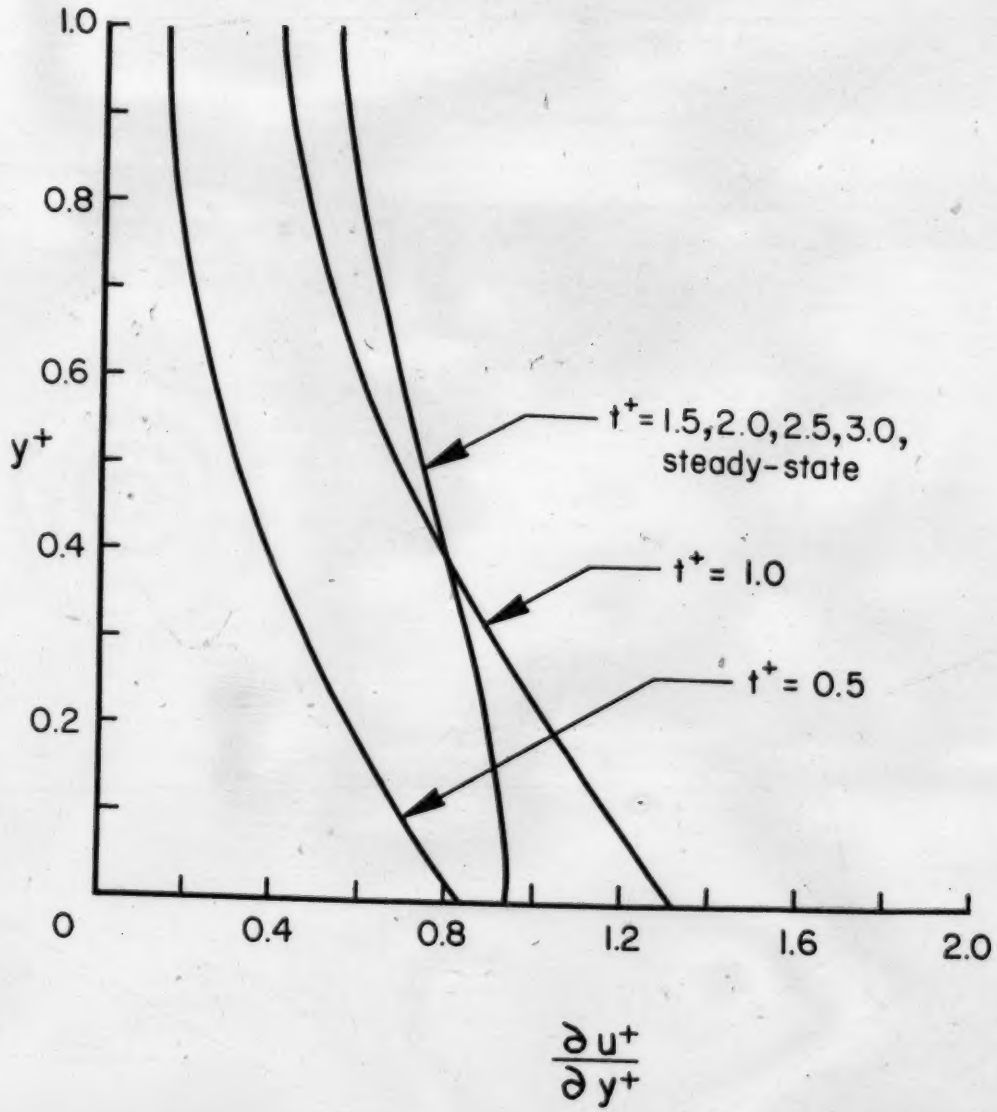

Fig. 21. Transient shear stress distribution at $x^+ = 0.7$ for K = 2.2

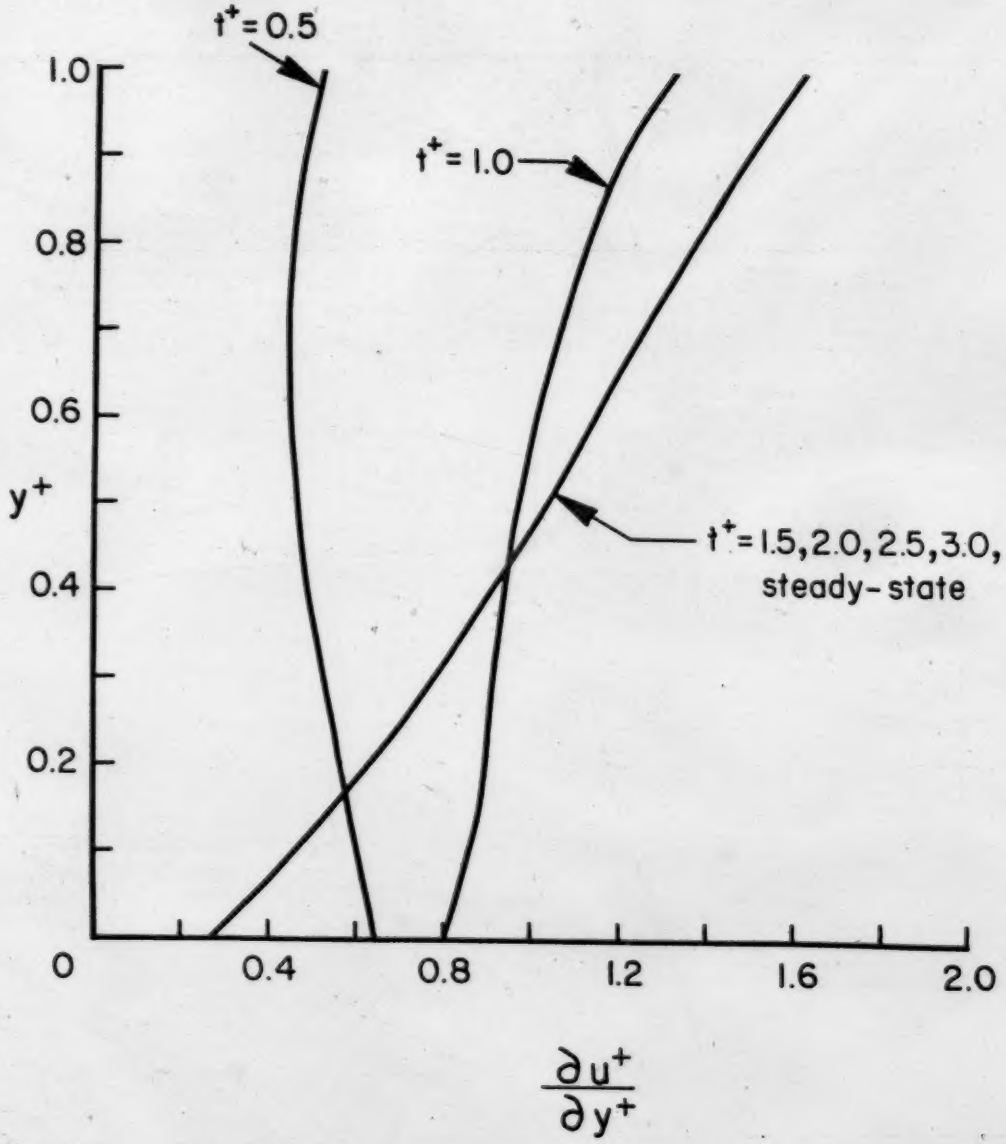

Fig. 22. Transient shear stress distribution at $x^+ = 1.0$ for K = 2.2

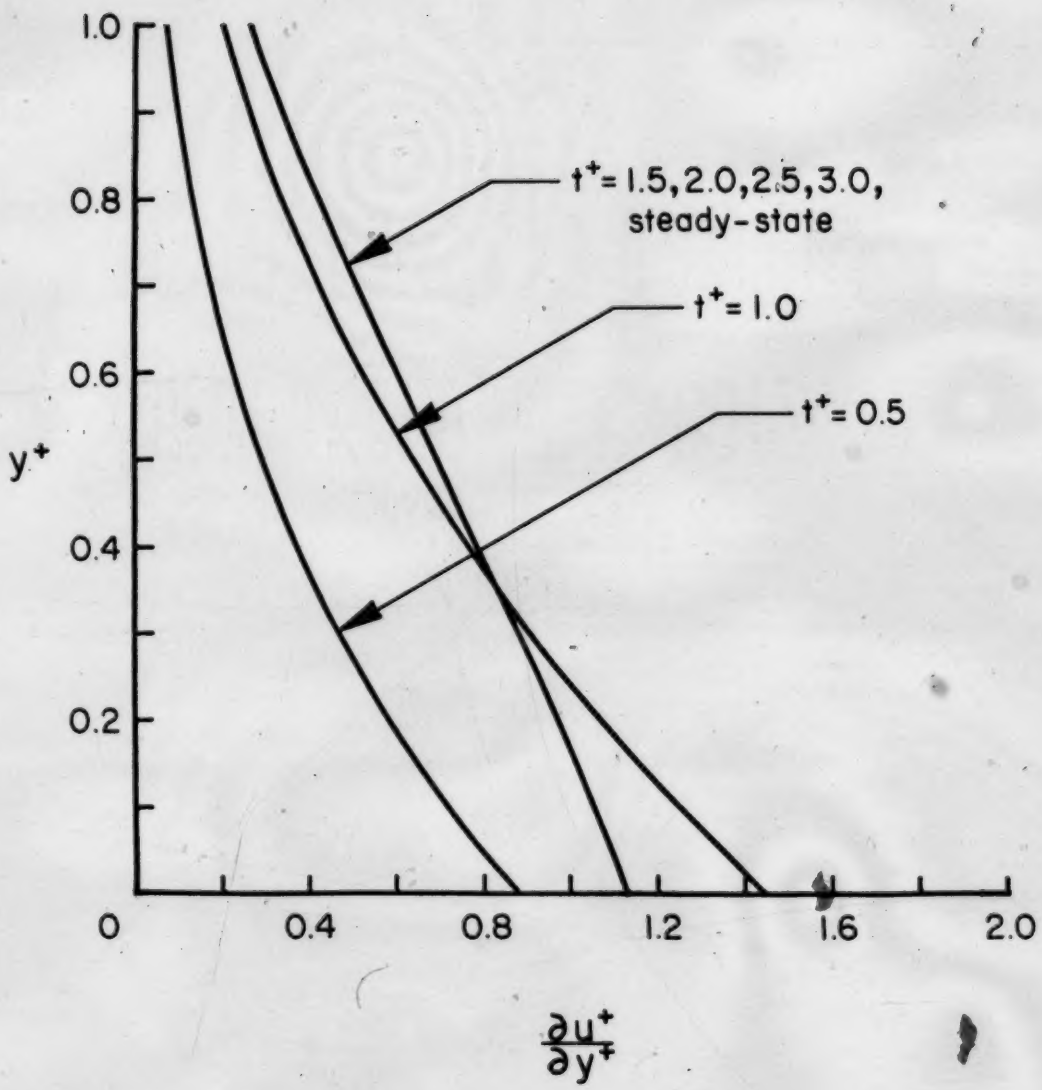

Fig. 23. Transient shear stress distribution at $x^+ = 0.1$ for K = 1.5

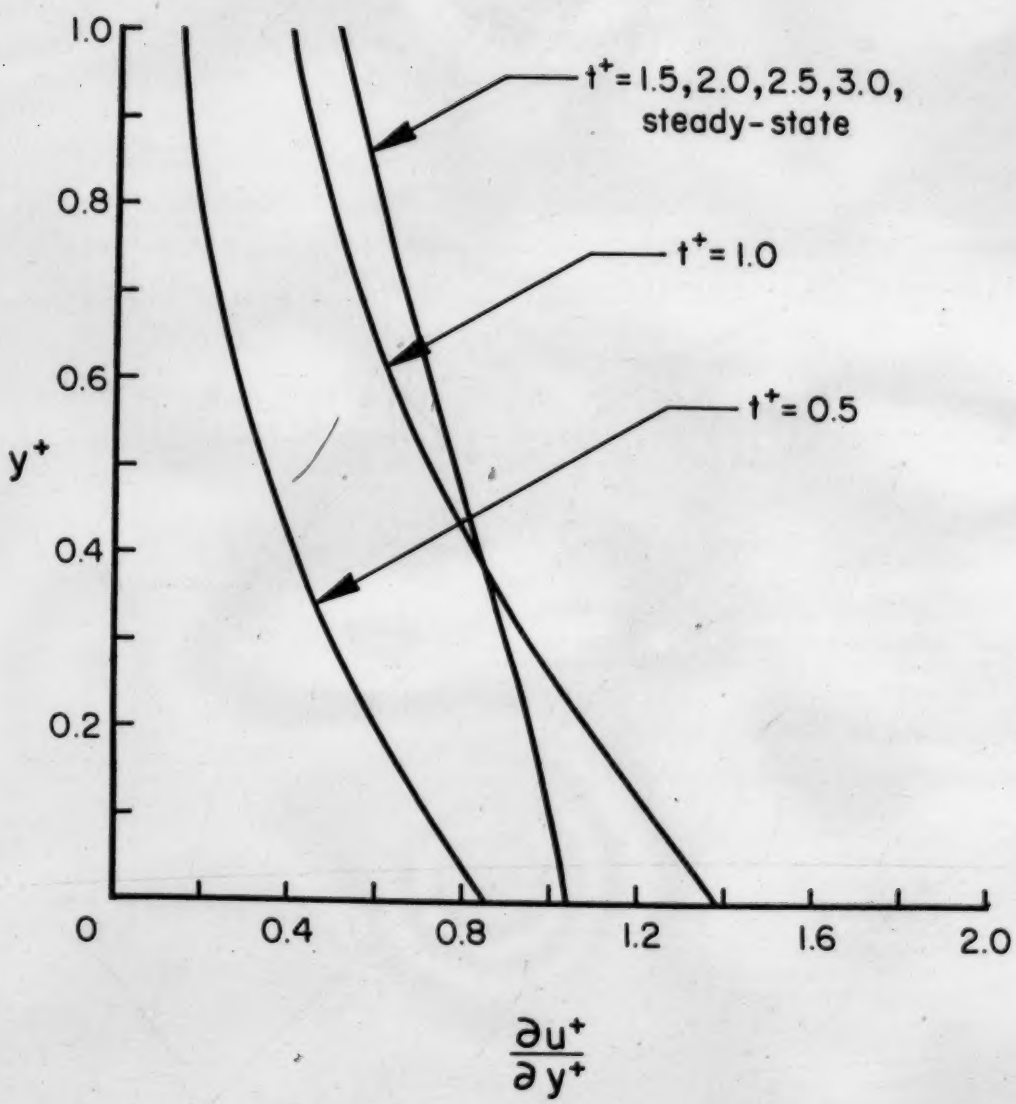

Fig. 24. Transient shear stress distribution at x'= 0.4 for K = 1.5

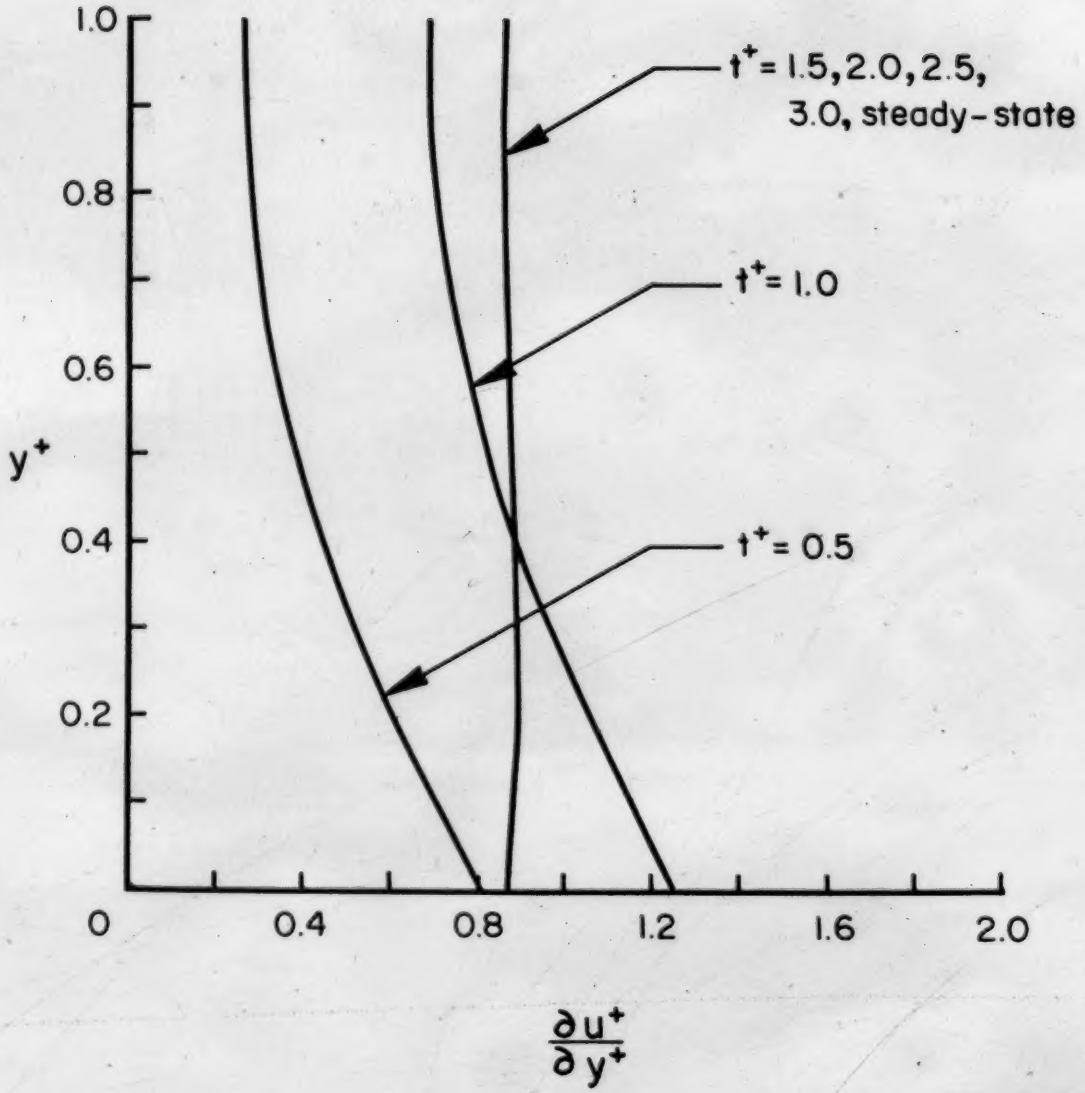

Fig. 25. Transient shear stress distribution at $x^+ = 0.7$ for K = 1.5

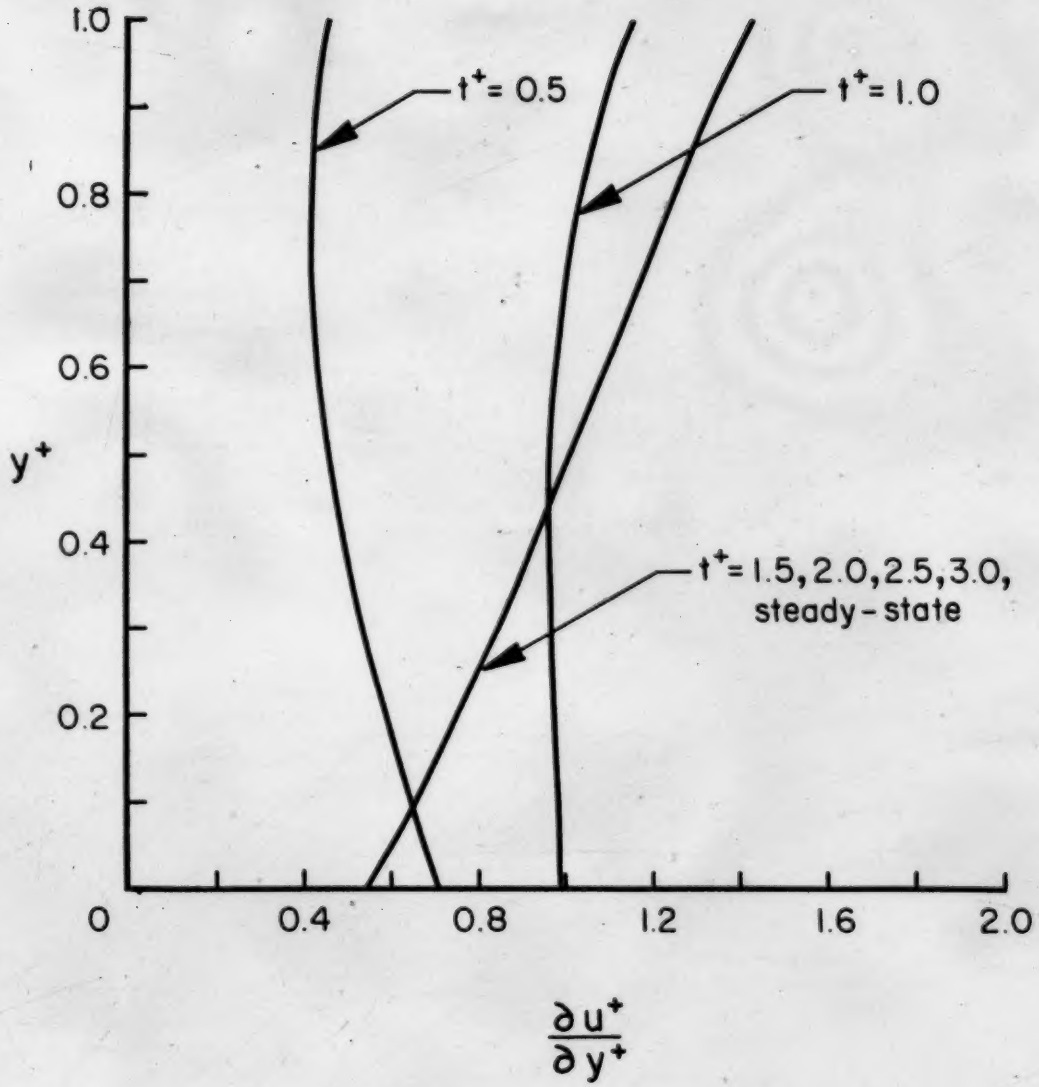

Fig. 26. Transient shear stress distribution at $x^+ = 1.0$ for K = 1.5

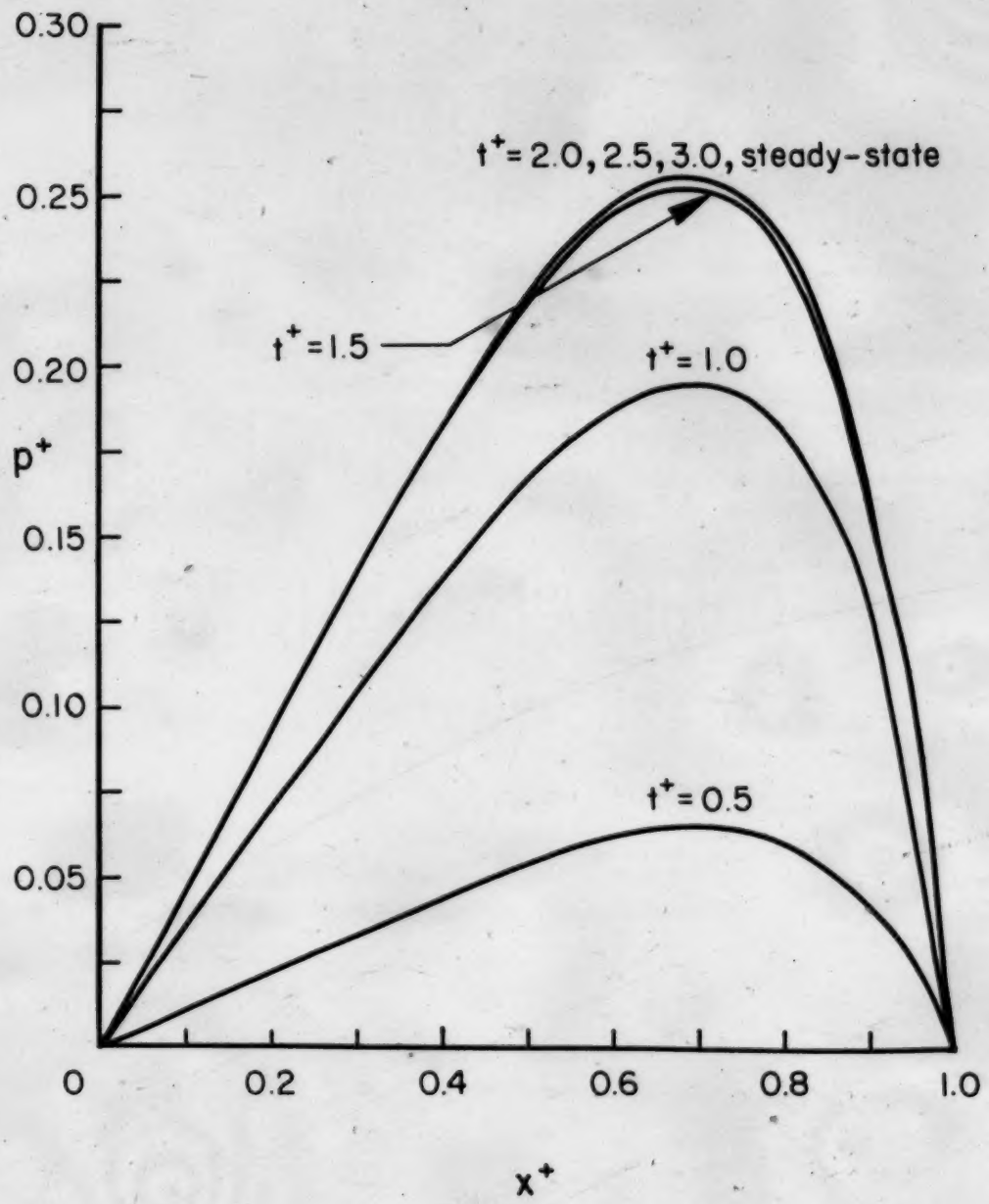

Fig. 27. Pressure distribution for K = 2.2

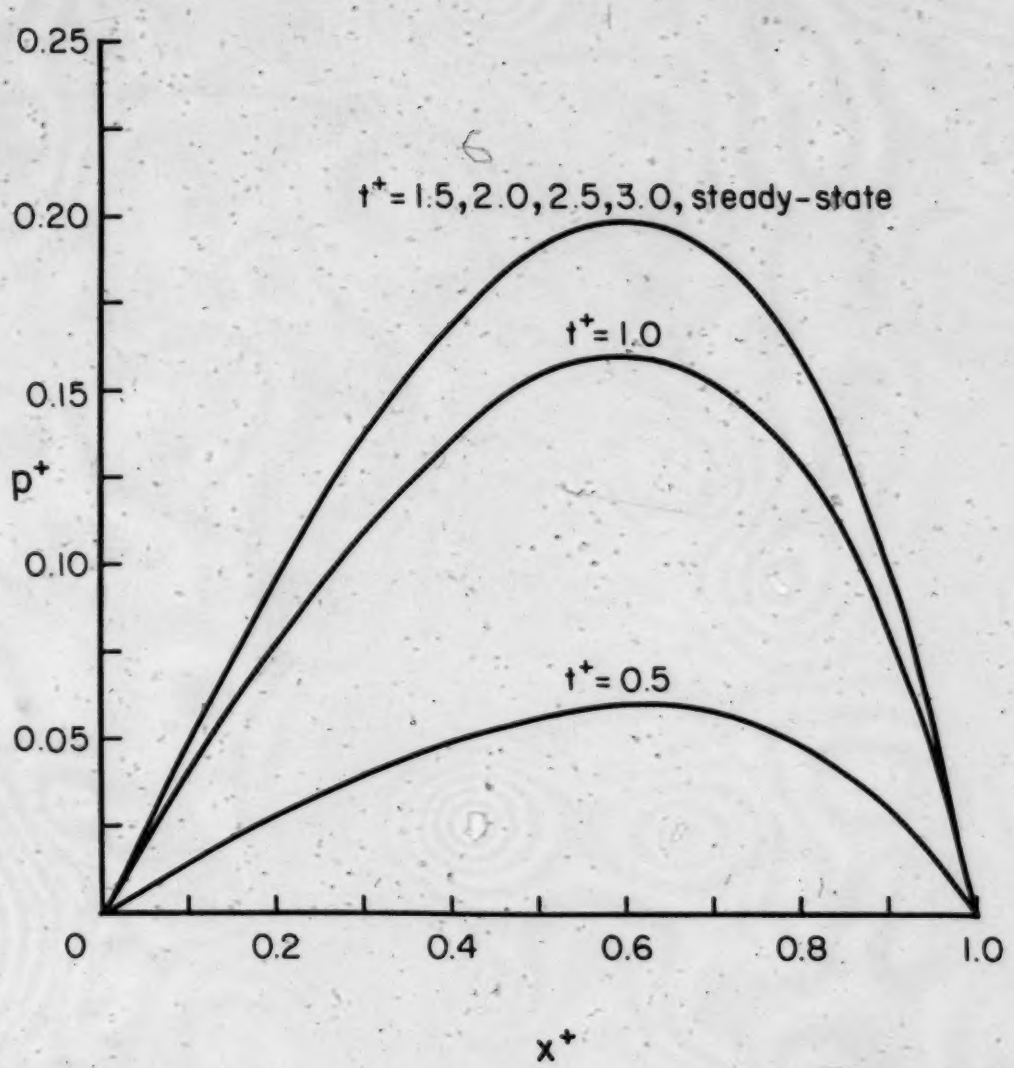

Fig. 28. Pressure distribution for K = 1.5

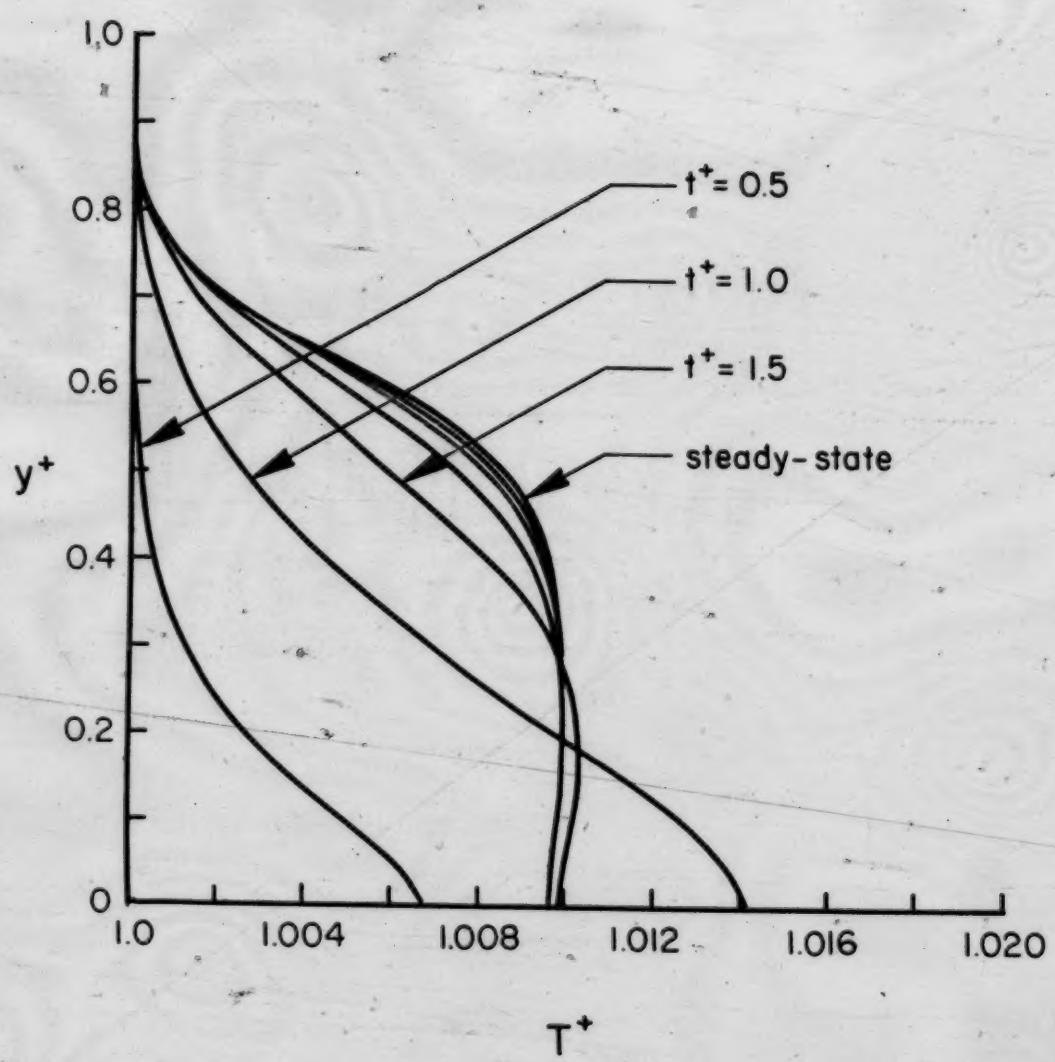

Fig. 29. Transient temperature distribution at x+= 0.1 for K = 2.2 (adiabatic slider)

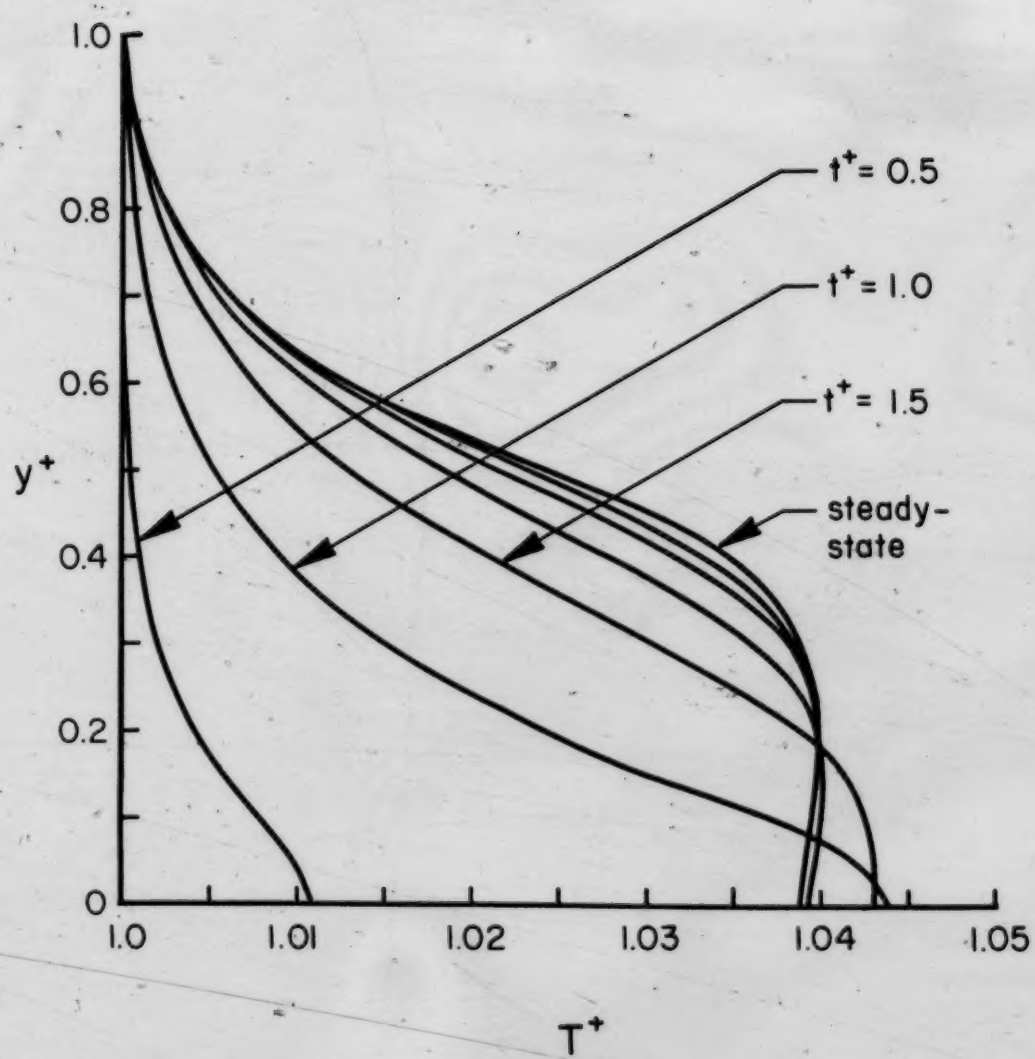

Fig. 30. Transient temperature distribution at $x^+ = 0.4$ for $K = 2.2$ (adiabatic slider)

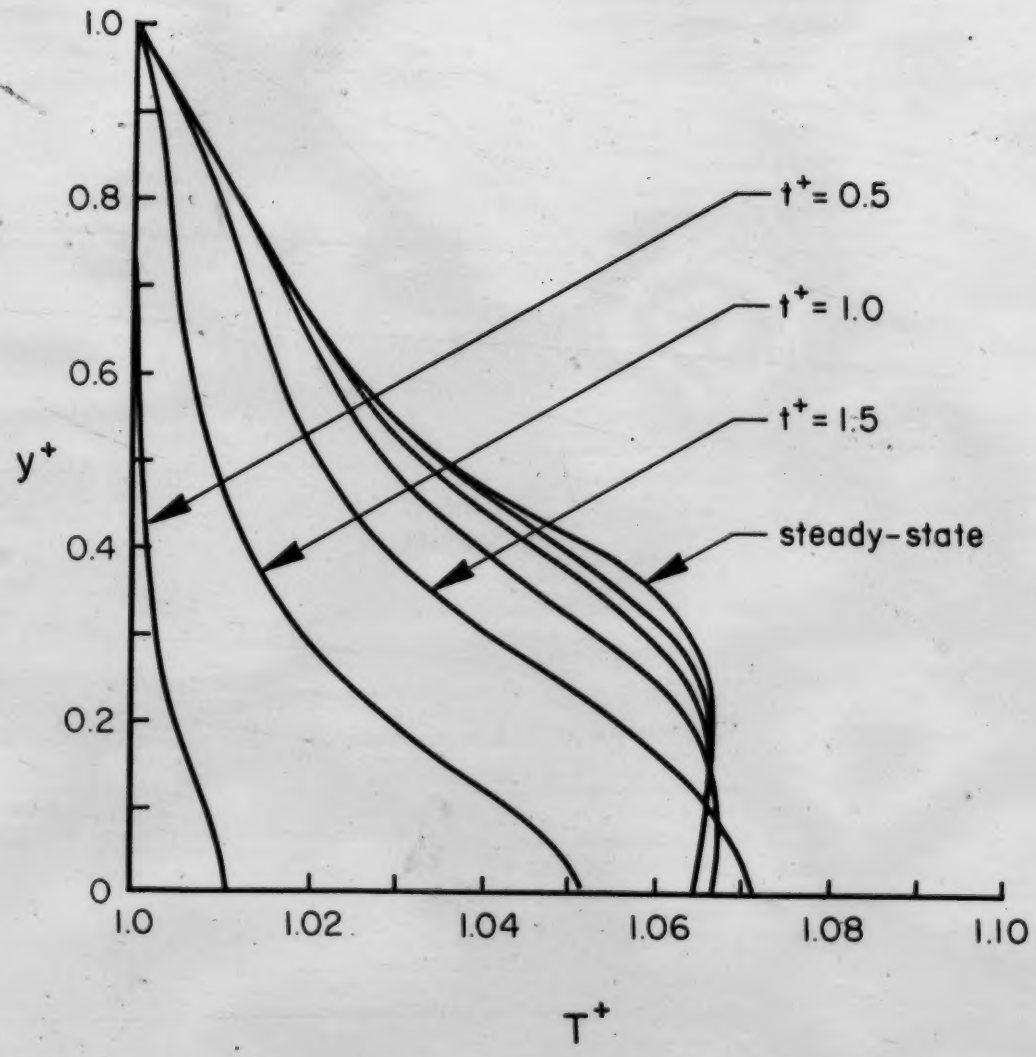

Fig. 31. Transient temperature distribution at $x^+ = 0.7$ for $K = 2.2$ (adiabatic slider)

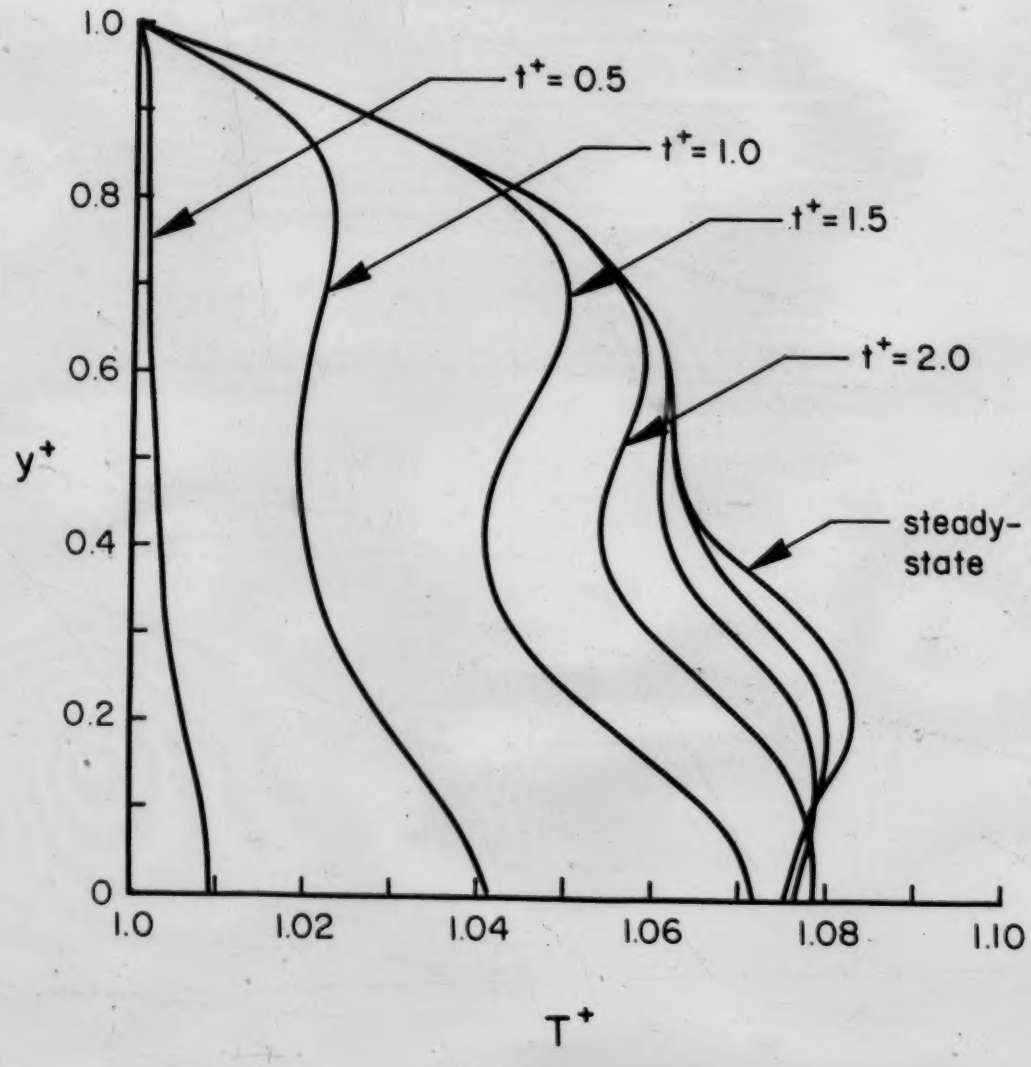

Fig. 32. Transient temperature distribution at $x^+ = 1.0$ for $K = 2.2$ (adiabatic slider)

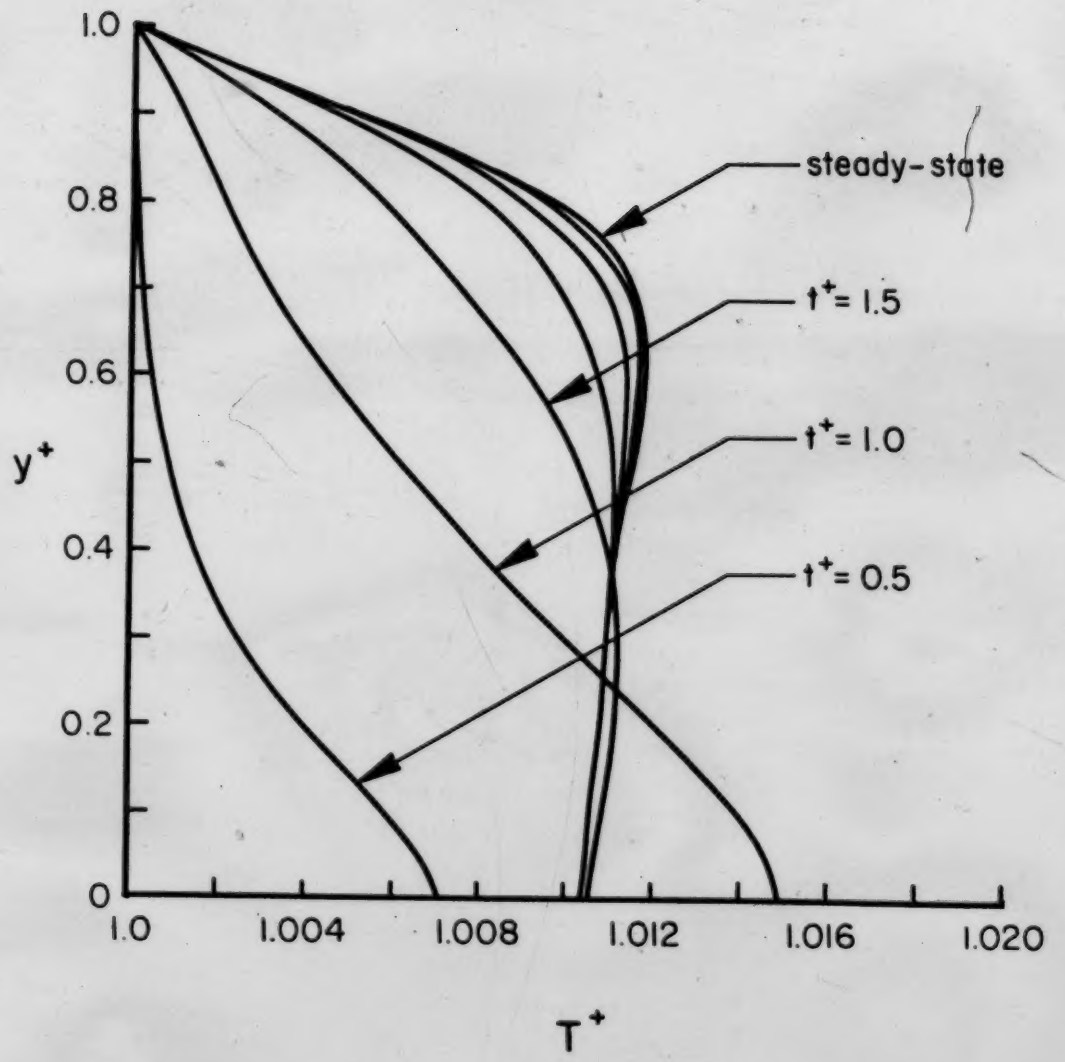

Fig. 33. Transient temperature distribution at $x^+ = 0.1$ for $K = 1.5$ (adiabatic slider)

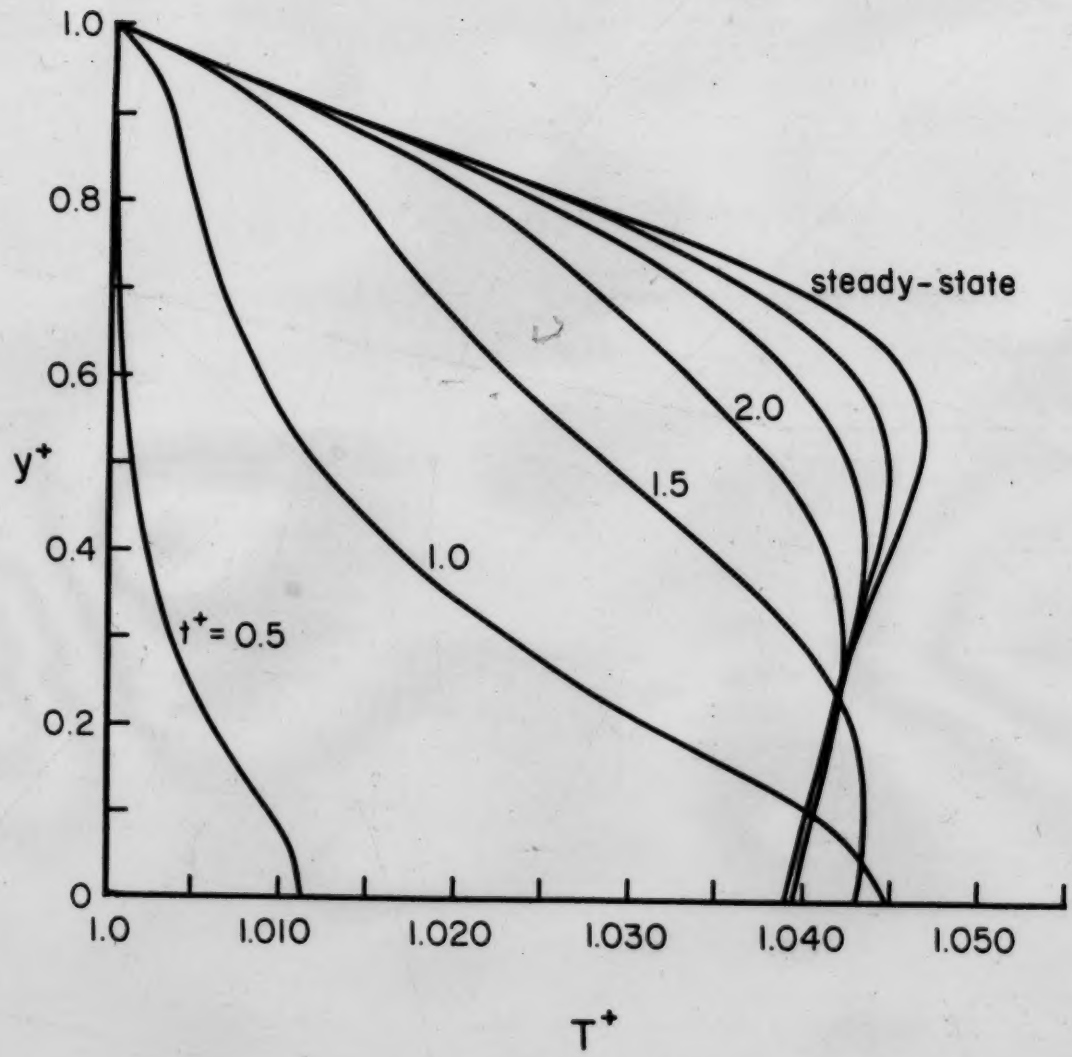

Fig. 34. Transient temperature distribution at $x^+ = 0.4$ for $K = 1.5$ (adiabatic slider)

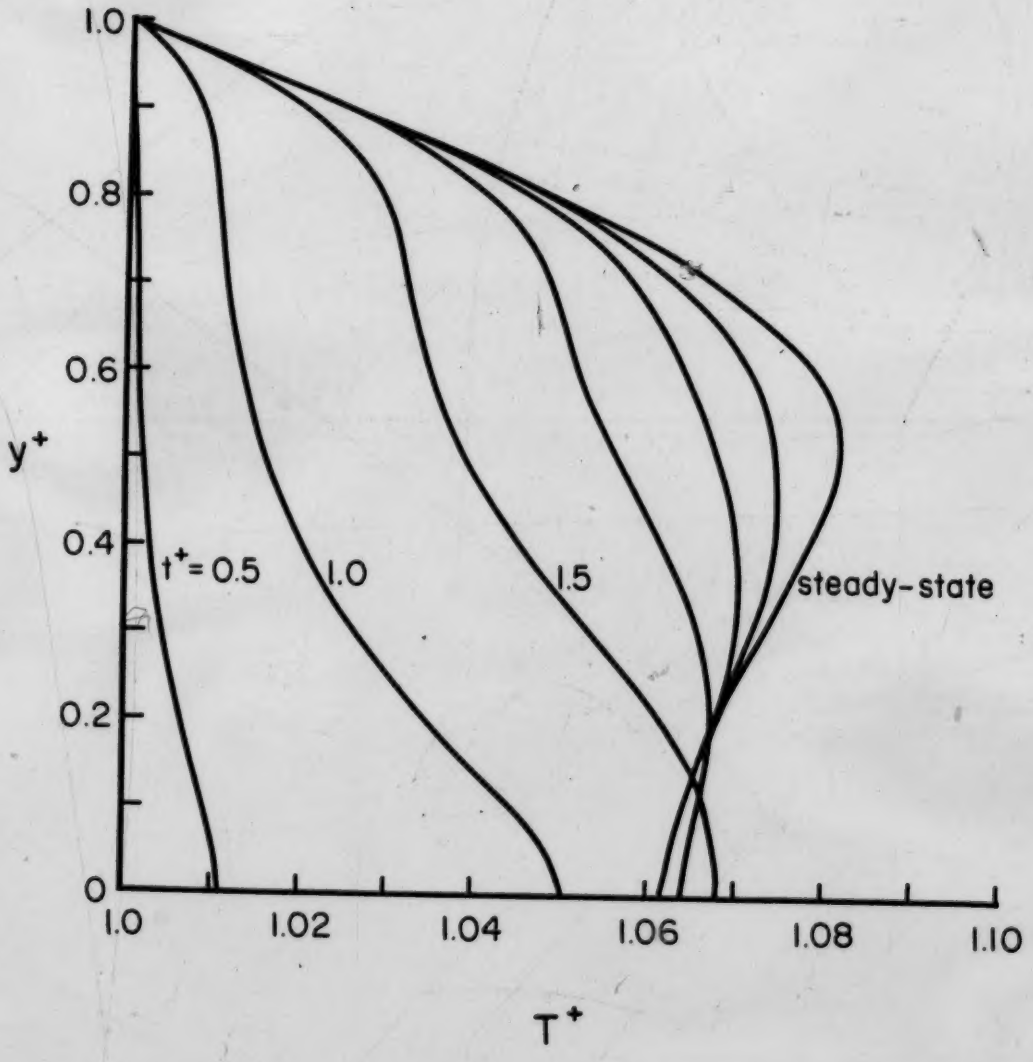

Fig. 35. Transient temperature distribution at x'= 0.7 for K = 1.5 (adiabatic slider)

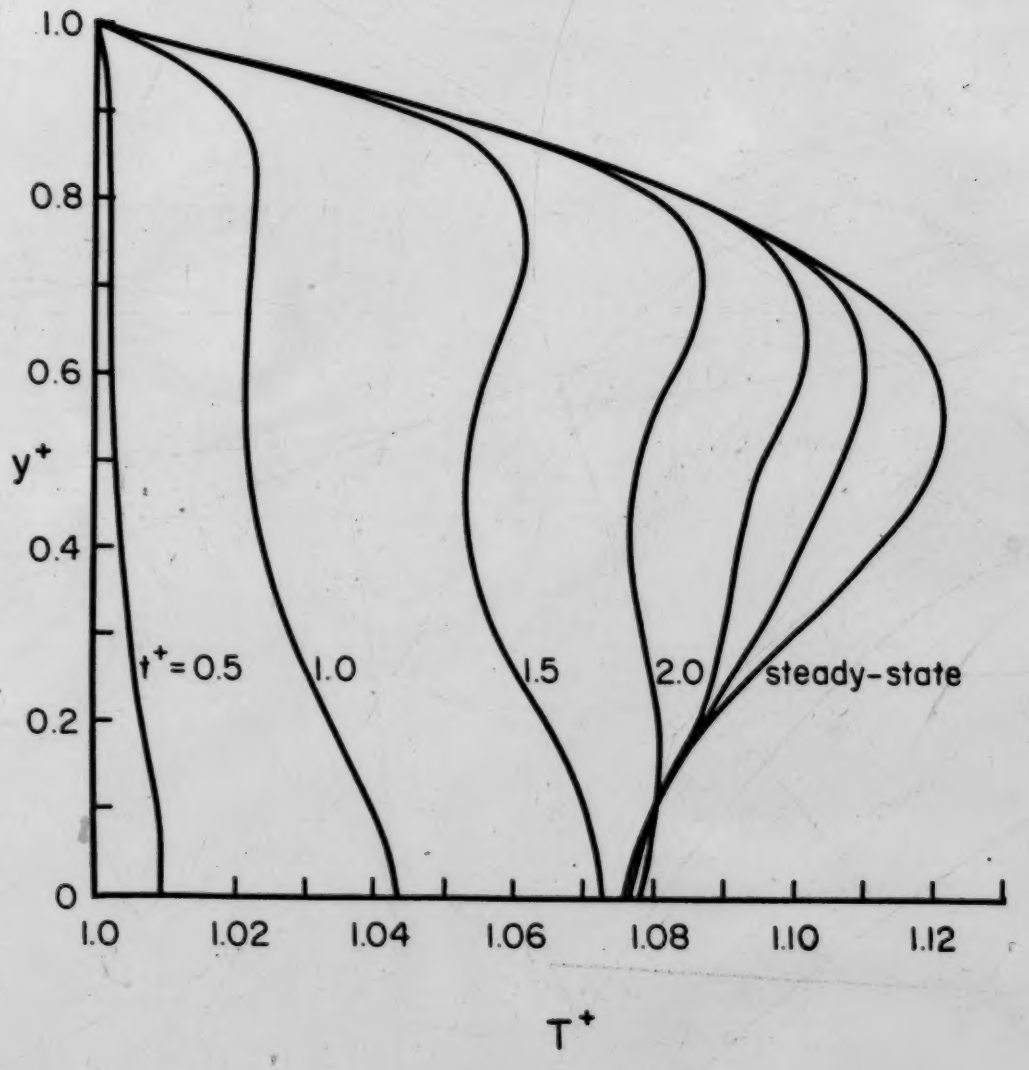

Fig. 36. Transient temperature distribution at $x^+ = 1.0$ for $K = 1.5$ (adiabatic slider)

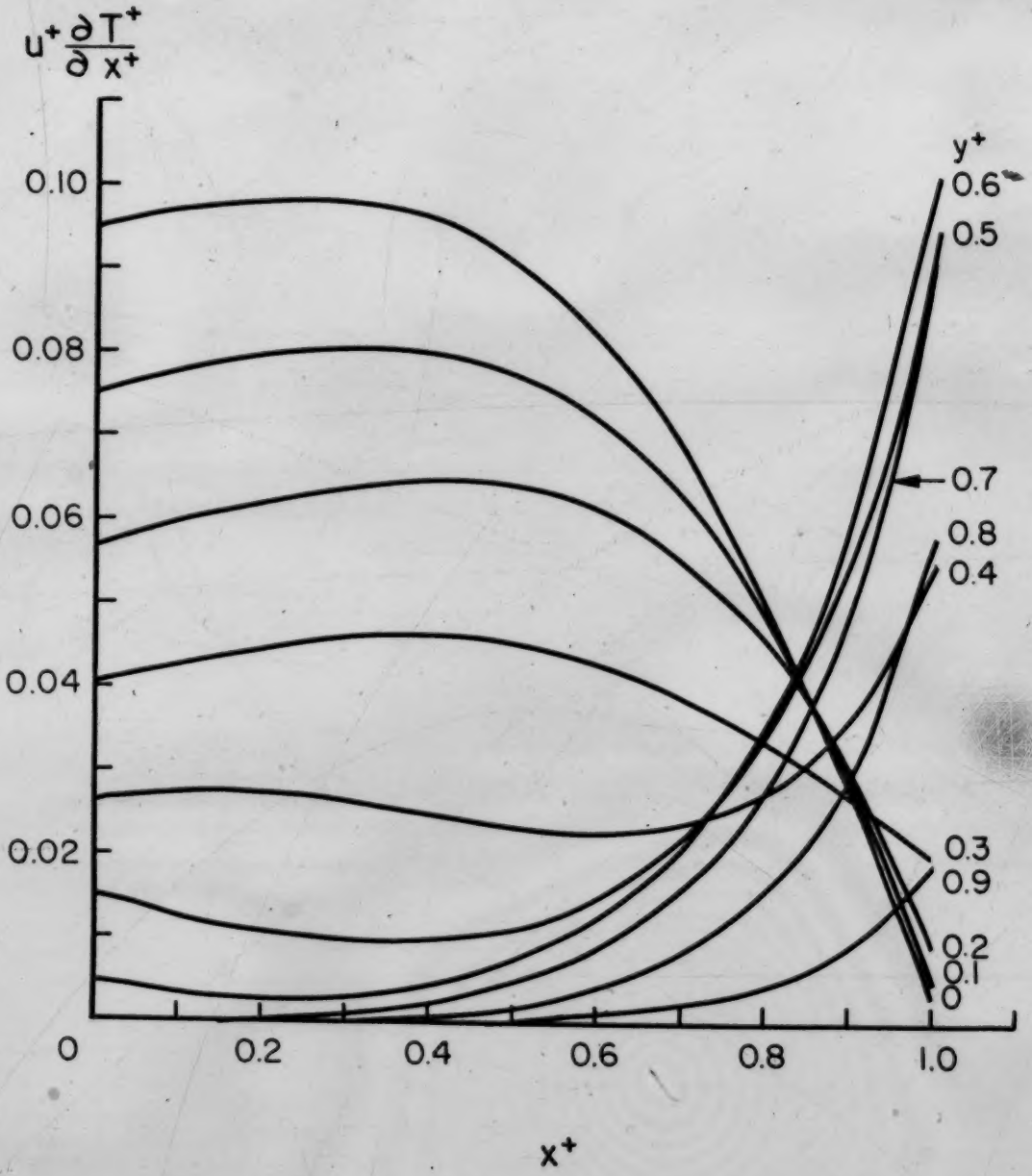

Fig. 37. Convection term along bearing as a function of y^+ ($t^+ = 3.0$, $K = 2.2$, adiabatic case)

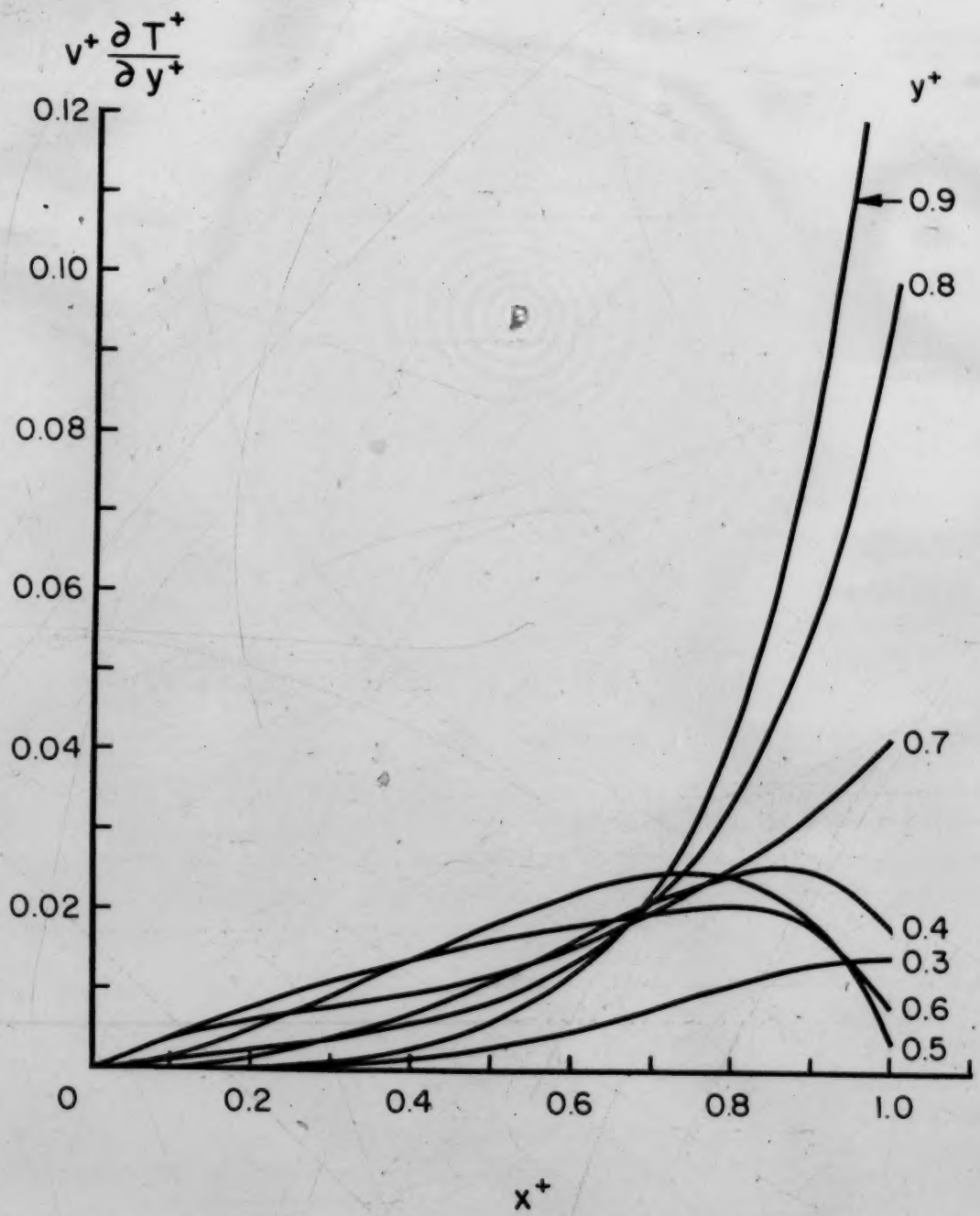

Fig. 38. Convection term across bearing as a function of y^+ ($t^+ = 3.0$, $K = 2.2$, adiabatic case)

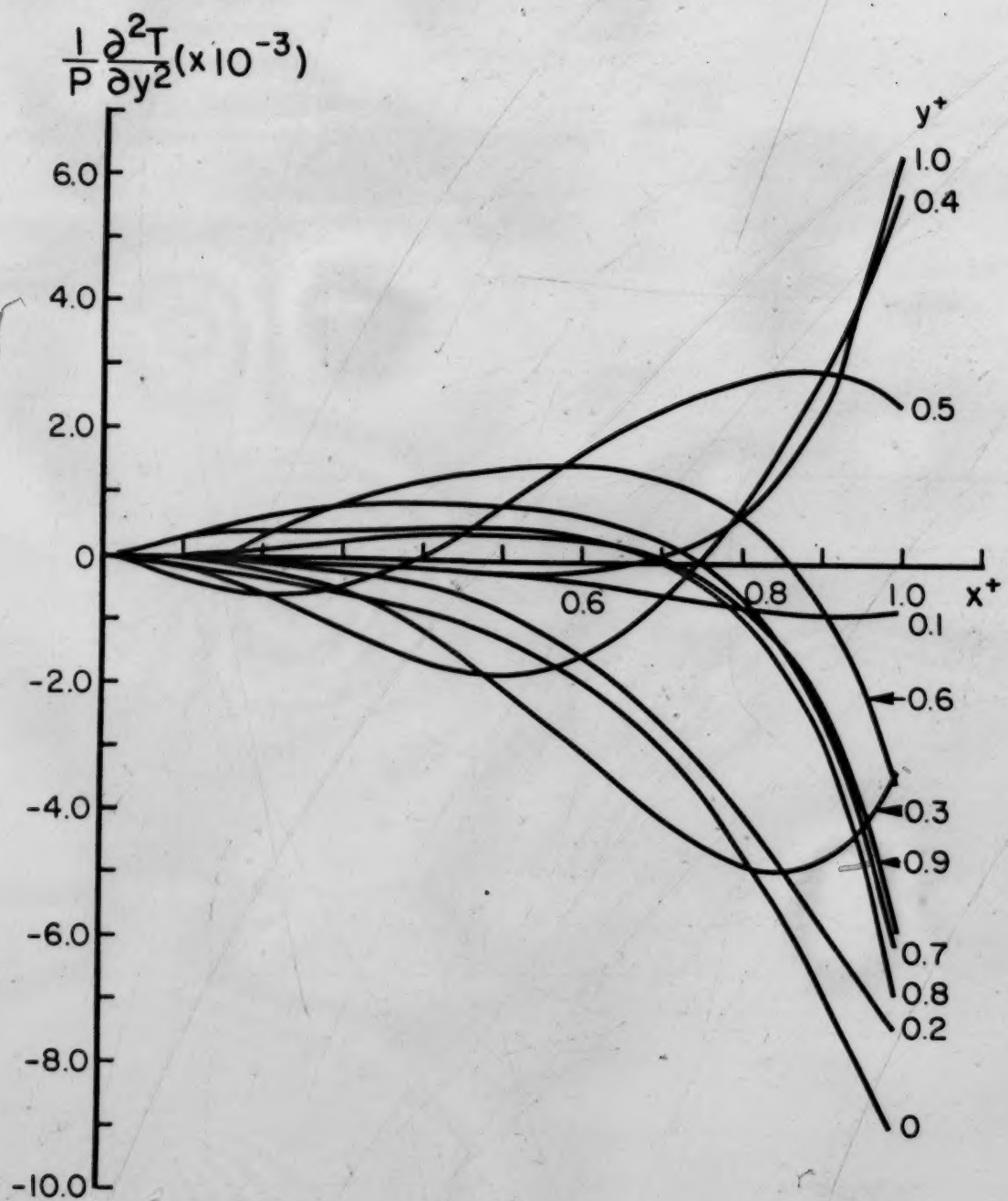

Fig. 39. Conduction term as a function of y^+ ($t^+ = 3.0$, $K = 2.2$, adiabatic case)

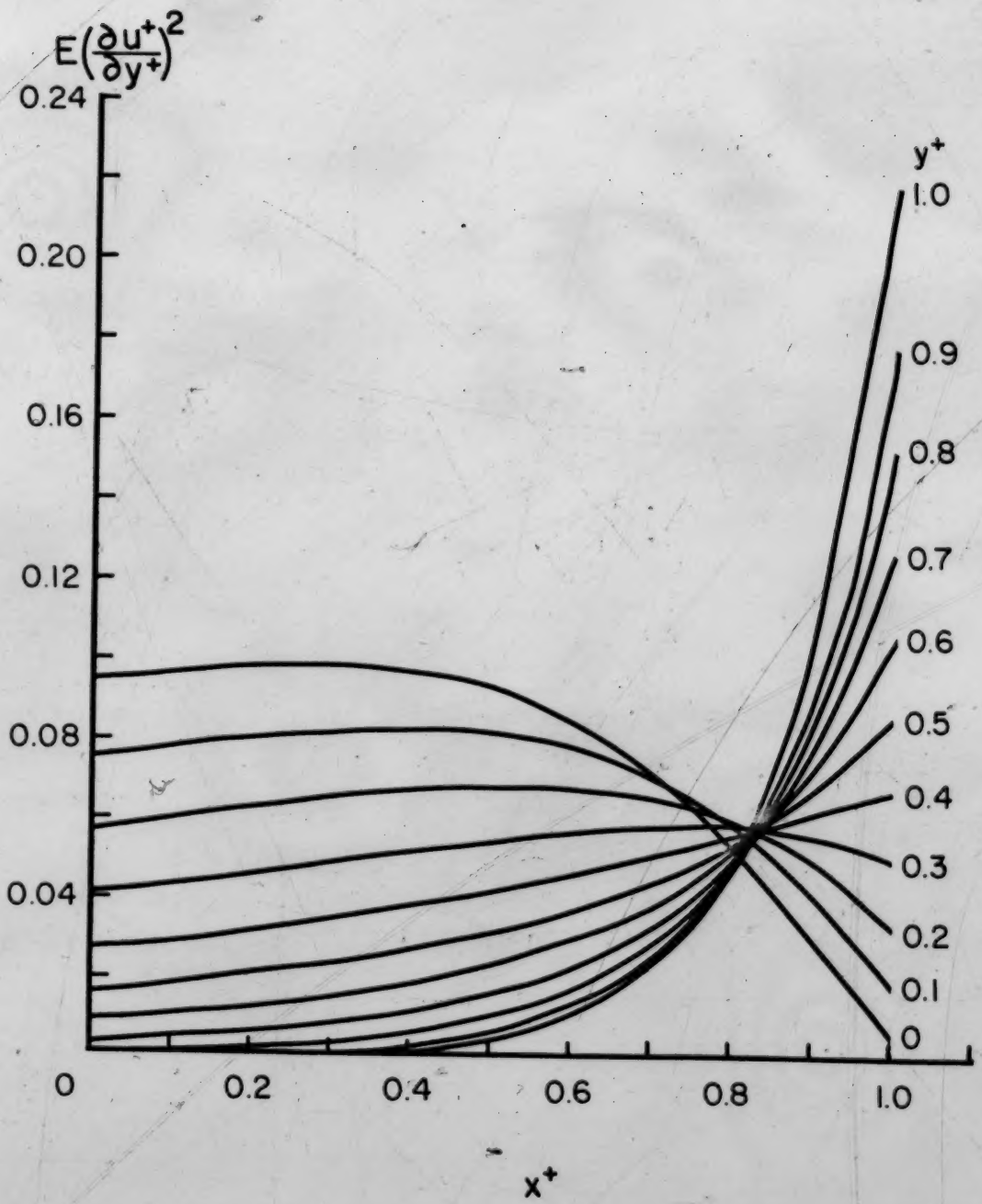

Fig. 40. Viscous term as a function of y^+ ($t^+ = 3.0$, $K = 2.2$, adiabatic case)

REFERENCES

1. Hahn, E. J., and Kettleborough C. F., Solution for the Pressure and Temperature in an Infinite Slider Bearing of Arbitrary Profile, *Journal of Lubrication Technology*, **89**, 445-452, 1967.

2. Rodkiewicz, C. M., and Anwar, M. I., Inertia and Convective Effects in Hydrodynamic Lubrication of a Slider Bearing,*Journal of Lubrication Technology*, **93**, 313-315, 1971.

3. Rodkiewicz, C. M., Hinds, J. C., and Dayson, C., The Thermally Boosted Oil Lubricated Sliding Thrust Bearing, *Journal of Lubrication Technology*, **96**, 322-328, 1974.

4. Hall, P. W., and Neal, P. B., Thermo-hydrodynamic Analysis of the Finite Slider Pad - Adiabatic Conditions, *International Journal of Mechanical Sciences*, 17 59-71, 1975.

5. Launder, B. E., and Leschziner, M., Flow in Finite-width Thrust Bearings Including Inertial Effects, *Journal of Lubrication Technology*, **100**, 330-338, 1978.

6. Ladanyi, D. J., Effects of Temporal Tangential Bearing Acceleration on Performance Characteristics of Slider and Journal Bearings, *NACA TN No. 1730*, 1948.

7. Lyman, F. A., and Saibel, E. A., Transient Lubrication of an Accelerated Infinite Slider, *ASLE Transactions*, **4**, 109-115, 1961.

8. Venkateswarlu, K., and Rodkiewicz, C. M., Thrust Bearing Characteristics when the Slider is Approaching Terminal Speed, *Wear*, **67**, 341-350, 1981.

9. Rodkiewicz, C. M., Venkateswarlu, K., and Gupta, R. N., Thrust Bearings in Time-dependent Laminar Flow, *Wear*, **63**, 381-391, 1980.

10. Vargaftik, N. B., *Tables of Thermophysical Properties of Liquids and Gases*, John Wiley & Sons, New York, 705-707, 1975.

11. Neale, M. J.,*Tribology Handbook* , Butterworths, London, 1973.

12. Oberg, E., and Jones, F. D., *Machinery's Handbook*, Industrial Press, New York, 1971.

BIBLIOGRAPHY

Baumeister, T., Editor-in-chief, *Mark's Standard Handbook for Mechanical Engineers*, McGraw-Hill, New York, 1978.

Chien, J. C., A General Finite-difference Formulation with Application to Navier-Stokes Equations, *Computers and Fluids*, 5, 15-31, 1977.

Gerald, C. F., *Applied Numerical Analysis*, Addison-Wesley, Massachusetts, 1978.

Hahn, E. J., and Kettleborough C. F., Solution for the Pressure and Temperature in an Infinite Slider Bearing of Arbitrary Profile, *Journal of Lubrication Technology*, 89, 445-452, 1967.

Hall, P. W., and Neal, P. B., Thermo-hydrodynamic Analysis of the Finite Slider Pad - Adiabatic Conditions, *International Journal of Mechanical Sciences*, 17, 59-71, 1975.

Ladanyi, D. J., Effects of Temporal Tangential Bearing Acceleration on Performance Characteristics of Slider and Journal Bearings, *NACA TN No. 1730*, 1948.

Launder, B. E., and Leschziner, M., Flow in Finite-width, Thrust Bearings Including Inertial Effects, *Journal of Lubrication Technology*, 100, 330-338, 1978.

Lyman, F. A., and Saibel, E. A., Transient Lubrication of an Accelerated Infinite Slider, *ASLE Transactions*, 4, 109-115, 1961.

Neale, M. J., *Tribology Handbook*, Butterworths, London, 1973.

Oberg, E., and Jones, F. D., *Machinery's Handbook*, Industrial Press, New York, 1971.

Raithby, G. D., and Torrance, K. E., Upstream-weighted Differencing Schemes and their Application to Elliptic Problems Involving Fluid Flow, *Computers and Fluids*, 2, 191-206, 1974.

Rodkiewicz, C. M., and Anwar, M. I., Inertia and Convective Effects in Hydrodynamic Lubrication of a Slider Bearing, *Journal of Lubrication Technology*, 93, 313-315, 1971.

Rodkiewicz, C. M., Hinds, J. C., and Dayson, C., The Thermally Boosted Oil Lubricated Sliding Thrust Bearing, *Journal of Lubrication Technology*, **96**, 322-328, 1974.

Rodkiewicz, C. M., Venkateswarlu, K., and Gupta, R. N., Thrust Bearings in Time-dependent Laminar Flow, *Wear*, **63**, 381-391, 1980.

Schlichting, H., *Boundary Layer Theory*, McGraw-Hill, New York, 1979.

Vargaftik, N. B., *Tables of Thermophysical Properties of Liquids and Gases*, John Wiley & Sons, New York, 1975.

Venkateswarlu, K., and Rodkiewicz, C. M., Thrust Bearing Characteristics when the Slider is Approaching Terminal Speed, *Wear*, **67**, 341-350, 1981.

Von Rosenburg, D. U., *Methods for the Numerical Solution of Partial Differential Equations*, American Elsevier, New York, 1975.